CSIAM Trans. Life Sci.
doi: 10.4208/csiam-ls.SO-2025-0015

Vol. **x**, No. x, pp. 1-45
xx 2025

Dynamics of Coral-Algae Phase Shifts via Ecological Stoichiometric Approach

Xin Zhao[1], Na Tian[2], Shiyang Yu[2,3] and Meng Fan[2,*]

[1] *Department of Mathematics, Harbin Institute of Technology (Weihai), Weihai 264209, P.R. China.*
[2] *Center for Mathematical Biosciences, School of Mathematics and Statistics, Northeast Normal University, Changchun 130024, P.R. China.*
[3] *College of Mathematics Science, Bohai University, Jinzhou 121013, P.R. China.*

Received 29 May 2025; Accepted 26 July 2025

On the auspicious occasion of celebrating the ninetieth birthday of Professor Zhien Ma, we extend our heartfelt congratulations and exporess our sincere gratitude for his profound contributions to the academic community.

Abstract. Coral reefs have evolved over hundreds of millions of years and are now considered one of the most critical yet vulnerable ecosystem on earth. Environmental changes, including variations in light availability, nutrient levels, and fishing pressure, can significantly impact the health of coral reefs, potentially leading to ecosystem degradation. A coral-macroalgae-herbivorous fish model is developed based on ecological stoichiometry to investigate the dynamics of coral-algae phase shifts. The positivity, invariance, and dissipativity of the model are carefully established, the existence and stability of equilibria are rigorously demonstrated, and rich dynamics such as bistability and various types of periodic oscillations are numerically explored. Furthermore, the effects of environmental factors (e.g., light intensity, nutrient levels, and fishing pressure) on the system's dynamics are investigated. The main findings highlight that environmental variations are key drivers of ecological phase transitions in coral reef ecosystems, providing more insights into the mechanisms underlying coral-algae dynamics and offering implications for the sustainable management of coral reefs.

AMS subject classifications: 92D25, 34F05, 92B05
Key words: Dynamic model, coral reef degradation, phase shifts, stability analysis, asymmetric dispersal.

1 Introduction

Coral reefs provide significant ecological and economic value, including sustaining marine biodiversity, protecting coastlines, and regulating the environment. In coral reef

---

*Corresponding author. *Email address:* `mfan@nenu.edu.cn` (M. Fan)

ecosystems, predation and competition are common ecological interactions that shape reef communities. Macroalgae and coral compete for essential resources such as light and space. Specifically, macroalgae form dense canopies that can shade the light required for photosynthesis, and their exudates can reduce coral calcification, thereby inhibiting coral growth [26, 31]. Corals can suppress macroalgae growth through mechanisms such as physical stimulation, chemical defense, and mucus secretion [34]. Moreover, macroalgae are grazed by herbivorous fish (e.g., parrotfish), a critical determinant of macroalgae biomass regulation in coral reef ecosystems [8, 12, 41]. The interspecific interactions among coral, macroalgae, and herbivorous fish are schematically illustrated in Fig. 1.

However, in recent decades, coral reefs have faced severe threats to their biodiversity, structure, and functionality, which is the result of the combined effects of human activities [57]. It is observed that coral reef degradation typically entails a phase shift in community structure, termed as a coral-algal phase shift, characterized by a decline in coral abundance corresponding to an increase in macroalgal abundance [9, 10, 27]. Ample evidence suggests that overfishing of herbivorous fish promotes the rapid growth of macroalgae [28, 42]. The expansion of macroalgae also suppresses coral settlement, disrupting the symbiotic relationship between coral polyps and their symbiotic algae. If such stress persists for an extended period, corals may experience large-scale mortality and eventual bleaching [32].

Many studies have developed dynamical models to understand the mechanisms driving coral-algae phase shifts. Early work by Mumby *et al.* [35] introduced a simplified model showing how reduced grazing could cause a loss of coral resilience and a shift to macroalgae dominance. Follow-up studies by Li *et al.* [25] and others [4,6,16,47,50,55,58, 59] further explored how overfishing, competition, and habitat degradation affect coral resilience. These models, however, primarily focus on trophic interactions without considering nutrient constraints. In addition, the combined effects of factors such as storm frequency, other physical disturbances, ocean warming, and acidification on coral-algae interactions have been investigated [1, 5, 14]. Sarkar *et al.* [41] utilized the continuous-time food chain models to study the impact of herbivorous fish harvesting on coral-algae phase shifts. Their findings suggest that reducing the harvesting rate of herbivorous fish

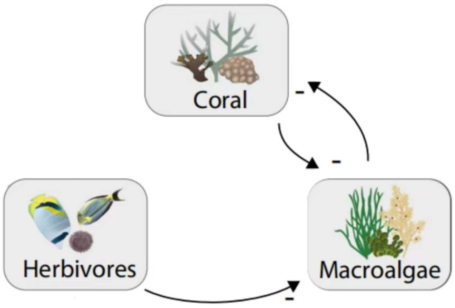

Figure 1: Schematic diagram illustrating the interactions among corals, macroalgae, and herbivorous fish [48].

can facilitate coral reef recovery. Furthermore, other scholars have explored the complex mechanisms underlying ecological phase transitions in coral reefs [3,46,52]. For instance, González-Rivero *et al.* [18] pointed out that, under certain conditions, the presence of macroalgae may enhance the recovery efficiency required to sustain coral communities, thereby delaying coral degradation.Models based on extended community composition have been used to evaluate the resilience of corals under single or multiple stressors. Despite substantial progress in modeling coral-algae phase shifts, certain influencing factors remain underexplored. For example, while existing studies often integrate macroalgal dynamics with those of herbivorous fish, they typically overlook the role of nutrient heterogeneity in shaping the cellular composition of macroalgae [6, 41]. In reality, nutrients such as nitrogen and phosphorus impose significant constraints on macroalgal growth, spatial competition, and ecological interactions within ecosystems [23]. More recently, some studies have begun integrating ecological stoichiometry into food web and algae-grazer models [2, 20, 22, 44]. Notably, Loladze *et al.* [29] introduced the Loladze-Kuang-Elser (LKE) model to reflect the role of food quality and nutrient limitation in consumer dynamics. Building on this, various stoichiometric models have been developed to study planktonic systems in freshwater [15, 19, 21, 30], highlighting how imbalanced nutrient content can destabilize ecosystems. Some efforts have extended this perspective to aquatic ecosystems including coral reefs [7, 11, 49], recognizing the importance of nutrient-to-carbon ratios in shaping trophic interactions. Despite these advances, stoichiometric approaches are rarely used in coral reef models. In particular, most models do not capture how nutrient heterogeneity, especially nitrogen availability, limits macroalgal growth and affects herbivorous fish via food quality. Furthermore, the combined effects of light, nutrients, and harvesting remain underexplored within a unified framework.

Despite significant progress in modeling coral reef ecosystems, existing approaches often neglect key nutrient constraints and fail to reflect the complex interplay between ecological and stoichiometric processes. In particular, most previous models are very restrictive to capture how nutrient heterogeneity (especially nitrogen availability) influences macroalgal growth and food quality for herbivorous fish. Moreover, environmental stressors such as light limitation and fishing pressure are often treated in isolation, without integrating their synergistic effects with stoichiometric constraints. These limitations hinder our ability to accurately describe phase transitions and resilience thresholds in coral-algae dynamics. Therefore, our study develops a novel stoichiometric modeling framework that captures both energy and nutrient limitations in coral reef ecosystems. The main contributions of this study are summarized as follows:

1. A novel coral-macroalgae-herbivorous fish model is proposed by incorporating ecological stoichiometry, where nutrient conservation laws and nitrogen-to-carbon ratios are explicitly considered to capture the effects of nutrient heterogeneity on macroalgal growth and food quality for herbivorous fish.
2. The model is rigorously analyzed in terms of positivity, boundedness, dissipativity, and the existence and stability of multiple equilibria. Conditions for global asymptotic stability and extinction are also derived under various ecological scenarios.

3. Rich dynamical behaviors, such as bistability, periodic oscillations, and threshold-driven regime shifts, are identified through numerical simulations. The model further investigates how variations in light intensity, nutrient levels, and grazing pressure collectively influence the stability and resilience of coral reef ecosystems.

The tree of this paper is organized as following. In Section 2, a coral-macroalgae-herbivorous fish dynamic model is developed based on ecological stoichiometry. Section 3 explores the system's positivity, dissipativity, and the existence and stability of equilibria. Section 4 presents the system's rich dynamical behaviors and investigates the effects of light intensity, nutrient levels, and grazing pressure on the population dynamics of corals, macroalgae, and herbivorous fish. Section 5 summarizes the key conclusions.

2 Model formulation

Sarkar *et al.* [41] established the following dynamic model:

$$\begin{cases} \dfrac{\mathrm{d}x}{\mathrm{d}t} = r_1 x\left(1-\dfrac{x}{K_1}\right) - g_1(y)x - f_1(x)z, \\ \dfrac{\mathrm{d}y}{\mathrm{d}t} = r_2 y\left(1-\dfrac{y}{K_2}\right) - g_2(x)y - f_2(y)z, \\ \dfrac{\mathrm{d}z}{\mathrm{d}t} = e_1 f_1(x)z + e_2 f_2(y)z - h(z)z - d_3 z, \end{cases} \tag{2.1}$$

assuming that, herbivorous fish primarily consume macroalgae, but they may also feed on corals to a limited extent. In (2.1), $x(t), y(t)$ and $z(t)$ represent the densities of corals, macroalgae, and herbivorous fish at time t, respectively; r_1 and r_2 denote the intrinsic growth rates of corals and macroalgae; K_1 and K_2 represent the environmental carrying capacities of corals and macroalgae, as influenced by light availability; $g_1(y)$ describes the inhibition, abrasion, and shading effects of macroalgae on coral growth; $g_2(x)$ represents the inhibitory effects of coral mechanisms, such as chemical defense and mucus secretion, on macroalgal growth [31]; $f_1(x)$ and $f_2(y)$ represent the functional responses of herbivorous fish to feeding on corals and macroalgae, respectively; e_1 and e_2 denote the maximum energy transfer efficiencies of herbivorous fish, which satisfy the second law of thermodynamics, i.e. $e_1 < 1, e_2 < 1$; $h(z)$ indicates the harvesting rate of herbivorous fish, and d_3 represents the natural mortality rate of herbivorous fish.

Based on (2.1), a model describing the interactions among corals, macroalgae, and herbivorous fish is established. For simplicity, this study only considers the grazing of macroalgae by herbivorous fish. Experimental observations by [36] indicate that the Holling II functional response better captures the behavior of herbivorous fish. Therefore, this study adopts the Holling II functional response, expressed as $f_2(y) = my/(b+y)$. It is noted that the competitive interaction between corals and macroalgae is limited, meaning that as the density of one species increases, its impact on the other species gradually saturates and ultimately stabilizes [41,51]. Therefore, the effects of inhibition and competition are modeled as

$$g_1(y)=\frac{c_1y}{(a_1+y)},\quad g_2(x)=\frac{c_2x}{(a_2+x)}.$$

Considering the losses incurred by corals and macroalgae due to external disturbances, it is assumed that the loss rates are constants [13,39]. Additionally, it is assumed that the harvesting of herbivorous fish is constant.

Based on the above assumptions, the following model is obtained:

$$\begin{cases}\dfrac{\mathrm{d}x}{\mathrm{d}t}=r_1x\left(1-\dfrac{x}{K_1}\right)-\dfrac{c_1xy}{a_1+y}-d_1x,\\ \dfrac{\mathrm{d}y}{\mathrm{d}t}=r_2y\left(1-\dfrac{y}{K_2}\right)-\dfrac{c_2xy}{a_2+x}-\dfrac{myz}{b+y}-d_2y,\\ \dfrac{\mathrm{d}z}{\mathrm{d}t}=\dfrac{emyz}{b+y}-hz-d_3z.\end{cases} \tag{2.2}$$

Now it is right position to establish the main model based on ecological stoichiometry. Since the growth of organisms is influenced by various nutrients, Odum and Odum [37] suggested that nitrogen (N) plays a key role in limiting coral reef ecosystems. Therefore, this study incorporates the effect of nitrogen on the system. Following the assumptions in [29] and combining them with real-world observations, the following assumptions are made.

Assumption 2.1. The total nitrogen in the system is constant, i.e. nitrogen is conserved, and its total amount is denoted as N (mg N/L).

Assumption 2.2. The nitrogen ratio in macroalgae biomass is variable but does not fall below a minimum value (q, mg N/mg C); the nitrogen ratios in coral biomass and herbivorous fish biomass remain constant and are denoted as θ_1 and θ_2 (mg N/mg C), respectively, where $q<\theta_2$ [38]. This is reasonable for most autotrophs and corresponding herbivorous organisms [24].

Assumption 2.3. The total nitrogen in the system is distributed across three components: corals, macroalgae, and herbivorous fish.

For (2.2), considering nitrogen conservation, the biomass of macroalgae is limited by both the environmental carrying capacity (energy limitation) and nitrogen availability. Assume that the nitrogen content in coral biomass is θ_1x and that in herbivorous fish biomass is θ_2z, then the nitrogen available for macroalgae is $N-\theta_1x-\theta_2z$. Since the nitrogen ratio in macroalgae biomass cannot be lower than q, the nitrogen-limited biomass of macroalgae is capped by $(N-\theta_1x-\theta_2z)/q$. Using Liebig's law of the minimum, which considers the joint limitations of environmental carrying capacity and nitrogen availability, the biomass of macroalgae is expressed as

$$\min\left(K_2,\frac{N-\theta_1x-\theta_2z}{q}\right). \tag{2.3}$$

The nitrogen-to-carbon (N:C) ratio in macroalgae is variable, and its actual N:C ratio is defined as $(N-\theta_1 x-\theta_2 z)/y$. If the N:C ratio in macroalgae exceeds that in herbivorous fish, it implies that the food quality (i.e. N:C ratio) consumed by the fish is sufficient to meet their nutritional needs. Under this condition, herbivorous fish can convert ingested food into biomass at their maximum conversion rate, with any excess nitrogen being excreted. Conversely, if the N:C ratio in macroalgae is lower than that in herbivorous fish, the fish must increase their food intake to compensate for the carbon deficit required for maintenance, resulting in a limitation of their maximum utilization efficiency and a reduction in their conversion rate. Assuming the conversion rate of herbivorous fish adheres to the principle of mass conservation, Liebig's law of the minimum dictates that the conversion rate is given by

$$e\min\left(1,\frac{(N-\theta_1 x-\theta_2 z)/y}{\theta_2}\right). \tag{2.4}$$

Based on the above discussion, by substituting (2.3) and (2.4) into (2.2), the ecological stoichiometric model illustrating the interaction among coral, macroalgae, and herbivorous fish is established and reads

$$\begin{cases} \dfrac{\mathrm{d}x}{\mathrm{d}t}=r_1 x\left(1-\dfrac{x}{K_1}\right)-\dfrac{c_1 xy}{a_1+y}-d_1 x, \\ \dfrac{\mathrm{d}y}{\mathrm{d}t}=r_2 y\left(1-\dfrac{y}{\min\left(K_2,(N-\theta_1 x-\theta_2 z)/q\right)}\right)-\dfrac{c_2 xy}{a_2+x}-\dfrac{myz}{b+y}-d_2 y, \\ \dfrac{\mathrm{d}z}{\mathrm{d}t}=e\min\left(1,\dfrac{(N-\theta_1 x-\theta_2 z)/y}{\theta_2}\right)\dfrac{myz}{b+y}-hz-d_3 z. \end{cases} \tag{2.5}$$

The biological significance, default value, and unit of parameters as well as references are provided in Table 1.

3 Main results

To better understand the dynamics of the proposed model, some fundamental mathematical properties are established first, including positivity, boundedness, and the existence and stability of equilibria.

Theorem 3.1. *The region*

$$\Delta=\{(x,y,z):0<x<K_1,0<y<k,0<z<N/\theta_2,qy+\theta_2 z<N\}$$

is positively invariant with respect to (2.5)*, where* $k=\min(K_2,N/q)$*.*

Proof. Let $A(t)=(x(t),y(t),z(t))$ be a solution of (2.5) satisfying the initial condition $A(0)\in\Delta$. Assume that there exists $t_1>0$ such that $A(t_1)$ reaches or crosses the boundary of Δ for the first time. The following cases are analyzed.

Table 1: Parameters in (2.5).

Notation	Biological significance	Value	Unit	Reference
r_1	Intrinsic growth rate of corals	0.5	day^{-1}	[57]
r_2	Intrinsic growth rate of macroalgae	0.6	day^{-1}	[54]
K_1	Carrying capacity of corals	0.7	mg C/m^2	[41]
K_2	Carrying capacity of macroalgae, limited by light	0.8	mg C/m^2	[41]
N	Total nitrogen concentration	0.5	mg C/m^3	[56]
q	Minimum nitrogen-to-carbon ratio in macroalgae	0.064	mg N/mg C	[56]
θ_1	Nitrogen-to-carbon ratio in corals	0.2	mg N/mg C	[17]
θ_2	Nitrogen-to-carbon ratio in herbivorous fish	0.2	mg N/mg C	[45]
c_1	Competition coefficient of macroalgae against corals	0.45	–	[41]
c_2	Competition coefficient of corals against macroalgae	0.2	–	[41]
a_1	Half-saturation coefficient for macroalgae competing with corals	0.3	mg C/m^2	[41]
a_2	Half-saturation coefficient for corals competing with macroalgae	0.3	mg C/m^2	–
m	Maximum grazing rate of herbivorous fish on macroalgae	1	$\text{day}^{-1}(\text{mg C/m}^2)^{-1}$	[41]
b	Half-saturation coefficient for herbivorous fish grazing on macroalgae	1.5	mg C/m^2	[41]
e	Maximum conversion efficiency of herbivorous fish	0.8	–	[41]
h	Maximum harvesting rate of herbivorous fish	0.15	day^{-1}	[41]
d_1	Loss rate of corals	0.02	day^{-1}	–
d_2	Loss rate of macroalgae	0.01	day^{-1}	–
d_3	Mortality rate of herbivorous fish	0.01	day^{-1}	[54]

(1) Assume that $x(t_1)=0$. Define

$$\bar{g}_1=\max_{t\in[0,t_1]}\frac{c_1y}{a_1+y}<\frac{c_1k}{a_1+k}.$$

For any $t\in[0,t_1]$, one has

$$\frac{\mathrm{d}x}{\mathrm{d}t}=r_1x\left(1-\frac{x}{K_1}\right)-\frac{c_1xy}{a_1+y}-d_1x$$

$$\geq -\frac{c_1xy}{a_1+y}-d_1x\geq -(\bar{g}_1+d_1)x\triangleq \alpha x,$$

where $\alpha=-(\bar{g}_1+d_1)$. By the comparison theorem, one obtains $x(t)\geq x(0)e^{\alpha t}$, which implies $x(t_1)\geq x(0)e^{\alpha t_1}>0$. This contradicts the assumption, and indicates that $A(t_1)$ cannot touch the boundary of Δ.

(2) Assume that $y(t_1)=0$. Define

$$\bar{g}_2=\max_{t\in[0,t_1]}\frac{c_2x}{a_2+x}<\frac{c_2K_1}{a_2+K_1},\quad \bar{z}=\max_{t\in[0,t_1]}z(t)<\frac{N}{\theta_2},\quad \frac{m}{b}=\max_{t\in[0,t_1]}\frac{m}{b+y}.$$

For any $t\in[0,t_1]$, one gets

$$\begin{aligned}\frac{\mathrm{d}y}{\mathrm{d}t}&=r_2y\left(1-\frac{y}{\min\big(K_2,(N-\theta_1x-\theta_2z)/q\big)}\right)-\frac{c_2xy}{a_2+x}-\frac{myz}{b+y}-d_2y\\&\geq -\frac{c_2xy}{a_2+x}-\frac{myz}{b+y}-d_2y\\&\geq -\left(\bar{g}_2+\frac{m}{b}\bar{z}+d_2\right)y\triangleq \beta y,\end{aligned}$$

where $\beta=-(g_2+m\bar{z}/b+d_2)$. By the comparison theorem, $y(t)\geq y(0)e^{\beta t}$, which implies $y(t_1)\geq y(0)e^{\beta t_1}>0$. This contradicts the assumption, and indicates that $A(t_1)$ cannot touch the boundary of Δ.

(3) Assume that $z(t_1)=0$. For any $t\in[0,t_1]$, one obtains

$$\begin{aligned}\frac{\mathrm{d}z}{\mathrm{d}t}&=e\min\left(1,\frac{(N-\theta_1x-\theta_2z)/y}{\theta_2}\right)\frac{myz}{b+y}-hz-d_3z\\&\geq -hz-d_3z\triangleq \gamma z,\end{aligned}$$

where $\gamma=-(h+d_3)$. By the comparison theorem, $z(t)\geq z(0)e^{\gamma t}$, which implies $z(t_1)\geq z(0)e^{\gamma t_1}>0$. This contradicts the assumption, and indicates that $A(t_1)$ cannot touch the boundary of Δ.

(4) Assume that $qy(t_1)+\theta_2z(t_1)=N$. For any $t\in[0,t_1]$, one gets $qy(t)+\theta_2z(t)<N$, then $qy'(t_1)+\theta_2z'(t_1)\geq 0$. Since

$$\begin{aligned}y'(t_1)=&\,r_2y(t_1)\left(1-\frac{y(t_1)}{\min\big(K_2,\big(N-\theta_1x(t_1)-\theta_2z(t_1)\big)/q\big)}\right)\\&-\frac{c_2x(t_1)y(t_1)}{a_2+x(t_1)}-\frac{my(t_1)z(t_1)}{b+y(t_1)}-d_2y(t_1)\\\leq&-\frac{c_2x(t_1)y(t_1)}{a_2+x(t_1)}-\frac{my(t_1)z(t_1)}{b+y(t_1)}-d_2y(t_1),\end{aligned}$$

$$\begin{aligned}z'(t_1)&=e\min\left(1,\frac{\big(N-\theta_1x(t_1)-\theta_2z(t_1)\big)/y(t_1)}{\theta_2}\right)\frac{my(t_1)z(t_1)}{b+y(t_1)}-hz(t_1)-d_3z(t_1)\\&\le e\frac{q}{\theta_2}\frac{my(t_1)z(t_1)}{b+y(t_1)},\end{aligned}$$

then

$$\begin{aligned}&qy'(t_1)+\theta_2z'(t_1)\\&\le -q\frac{c_2x(t_1)y(t_1)}{a_2+x(t_1)}-q\frac{my(t_1)z(t_1)}{b+y(t_1)}-qd_2y(t_1)+\theta_2e\frac{q}{\theta_2}\frac{my(t_1)z(t_1)}{b+y(t_1)}\\&\le(e-1)\frac{qmy(t_1)z(t_1)}{b+y(t_1)}-\frac{qc_2x(t_1)y(t_1)}{a_2+x(t_1)}-qd_2y(t_1).\end{aligned}$$

Notice that $e<1$, then $qy'(t_1)+\theta_2z'(t_1)<0$. This contradicts the assumption, and indicates that $A(t_1)$ cannot touch the boundary of Δ.

(5) Let $x(t_1)=K_1$. For any $t\in[0,t_1]$, one obtains

$$\begin{aligned}\frac{\mathrm{d}x}{\mathrm{d}t}&=r_1x\left(1-\frac{x}{K_1}\right)-\frac{c_1xy}{a_1+y}-d_1x\\&\le r_1x\left(1-\frac{x}{K_1}\right).\end{aligned}$$

By the comparison theorem, $x(t)\le K_1$, and $x(t_1)\le K_1$, which indicates that $A(t_1)$ cannot cross the boundary of Δ.

(6) Let $y(t_1)=k$. For any $t\in[0,t_1]$, one has

$$\begin{aligned}\frac{\mathrm{d}y}{\mathrm{d}t}&=r_2y\left(1-\frac{y}{\min\big(K_2,(N-\theta_1x-\theta_2z)/q\big)}\right)-\frac{c_2xy}{a_2+x}-\frac{myz}{b+y}-d_2y\\&\le r_2y\left(1-\frac{y}{\min\big(K_2,(N-\theta_1x-\theta_2z)/q\big)}\right)\\&\le r_2y\left(1-\frac{y}{\min(K_2,N/q)}\right)\\&=r_2y\left(1-\frac{y}{k}\right).\end{aligned}$$

By the comparison theorem, $y(t)\le k$, and $y(t_1)\le k$, which indicates that $A(t_1)$ cannot cross the boundary of Δ.

(7) Let $z(t_1)=N/\theta_2$. For any $t\in[0,t_1]$, one gets

$$\frac{\mathrm{d}z}{\mathrm{d}t}=e\min\left(1,\frac{(N-\theta_1x-\theta_2z)/y}{\theta_2}\right)\frac{myz}{b+y}-hz-d_3z$$

$$\begin{aligned}
&\le e\min\left(1,\frac{(N-\theta_1 x-\theta_2 z)/y}{\theta_2}\right)\frac{myz}{b+y}\\
&\le \frac{emz}{b+y}\frac{N-\theta_1 x-\theta_2 z}{\theta_2}\le\frac{emz}{b}\frac{N-\theta_2 z}{\theta_2}\\
&=\frac{emN}{b\theta_2}z\left(1-\frac{z}{N/\theta_2}\right).
\end{aligned}$$

By the comparison theorem, $z(t)\le N/\theta_2$, and $z(t_1)\le N/\theta_2$, which indicates that $A(t_1)$ cannot cross the boundary of Δ. In conclusion, any trajectory starting from Δ will eventually remain within Δ, which implies that Δ is positively invariant with respect to (2.5). The proof is complete. □

Theorem 3.2. *System* (2.5) *is dissipative.*

Proof. Let $R(t)=x(t)+y(t)+z(t)$, then

$$\begin{aligned}
\frac{\mathrm{d}R}{\mathrm{d}t}=&\,r_1x\left(1-\frac{x}{K_1}\right)-\frac{c_1xy}{a_1+y}-d_1x+r_2y\left(1-\frac{y}{\min\left(K_2,(N-\theta_1x-\theta_2z)/q\right)}\right)\\
&-\frac{c_2xy}{a_2+x}-\frac{myz}{b+y}-d_2y+e\min\left(1,\frac{(N-\theta_1x-\theta_2z)/y}{\theta_2}\right)\frac{myz}{b+y}-hz-d_3z\\
\le&\,r_1x\left(1-\frac{x}{K_1}\right)-d_1x+r_2y\left(1-\frac{y}{K_2}\right)-\frac{myz}{b+y}-d_2y+\frac{emyz}{b+y}-hz-d_3z\\
\le&\,r_1x-\alpha r_1x^2-d_1x+r_2y-\alpha r_2y^2-d_2y-hz-d_3z\\
=&\,(r_1-d_1+\beta)x-\alpha r_1x^2+(r_2-d_2+\beta)y-\alpha r_2y^2-\beta(x+y+z),
\end{aligned}$$

where $\alpha=\min\{1/K_1,1/K_2\},\beta=h+d_3$. Therefore,

$$\begin{aligned}
\frac{\mathrm{d}R}{\mathrm{d}t}+\beta R\le&\,(r_1-d_1+\beta)x-\alpha r_1x^2+(r_2-d_2+\beta)y-\alpha r_2y^2\\
=&-\alpha r_1\left(x-\frac{r_1-d_1+\beta}{2\alpha r_1}\right)^2+\frac{(r_1-d_1+\beta)^2}{4\alpha r_1}\\
&-\alpha r_2\left(y-\frac{r_2-d_2+\beta}{2\alpha r_2}\right)^2+\frac{(r_2-d_2+\beta)^2}{4\alpha r_2}\\
\le&\,\frac{r_2(r_1-d_1+\beta)^2+r_1(r_2-d_2+\beta)^2}{4\alpha r_1r_2}.
\end{aligned}$$

Integrating both sides yields

$$R(t)\le\frac{r_2(r_1-d_1+\beta)^2+r_1(r_2-d_2+\beta)^2}{4\alpha\beta r_1r_2}(1-e^{-\beta t})+R(0)e^{-\beta t}.$$

Then

$$\limsup_{t\to\infty} R(t) \le \frac{r_2(r_1-d_1+\beta)^2+r_1(r_2-d_2+\beta)^2}{4\alpha\beta r_1 r_2},$$

which implies that (2.5) is dissipative. □

For convenience of discussion, the following transformations are applied to (2.5):

$$\frac{N}{\theta_2} \to N, \quad \frac{\theta_1}{\theta_2} \to \theta_1, \quad \frac{q}{\theta_2} \to q.$$

Then

$$\begin{cases} \dfrac{\mathrm{d}x}{\mathrm{d}t} = r_1 x\left(1-\dfrac{x}{K_1}\right) - \dfrac{c_1 xy}{a_1+y} - d_1 x, \\ \dfrac{\mathrm{d}y}{\mathrm{d}t} = r_2 y\left(1-\dfrac{y}{\min\left(K_2,(N-\theta_1 x-z)/q\right)}\right) - \dfrac{c_2 xy}{a_2+x} - \dfrac{myz}{b+y} - d_2 y, \\ \dfrac{\mathrm{d}z}{\mathrm{d}t} = e\min\left(1,\dfrac{N-\theta_1 x-z}{y}\right)\dfrac{myz}{b+y} - hz - d_3 z. \end{cases} \tag{3.1}$$

Denote

$$\frac{\mathrm{d}x}{\mathrm{d}t} = xF(x,y,z), \quad \frac{\mathrm{d}y}{\mathrm{d}t} = yG(x,y,z), \quad \frac{\mathrm{d}z}{\mathrm{d}t} = zH(x,y,z), \tag{3.2}$$

where

$$\begin{aligned} F(x,y,z) &= r_1\left(1-\frac{x}{K_1}\right) - \frac{c_1 y}{a_1+y} - d_1, \\ G(x,y,z) &= r_2\left(1-\frac{y}{\min\left(K_2,(N-\theta_1 x-z)/q\right)}\right) - \frac{c_2 x}{a_2+x} - \frac{mz}{b+y} - d_2, \\ H(x,y,z) &= e\min\left(1,\frac{N-\theta_1 x-z}{y}\right)\frac{my}{b+y} - h - d_3. \end{aligned}$$

The positive invariant set of (3.1) is

$$\Delta^* = \{(x,y,z) : 0<x<K_1, 0<y<k, 0<z<N/\theta_2, qy+z<N\},$$

where $k = \min(K_2, N/q)$.

Straightforward algebraic calculation leads to the following Jacobian matrix of (3.1):

$$J(x,y,z) = \begin{pmatrix} F+xF_x(x,y,z) & xF_y(x,y,z) & xF_z(x,y,z) \\ yG_x(x,y,z) & G+yG_y(x,y,z) & yG_z(x,y,z) \\ zH_x(x,y,z) & zH_y(x,y,z) & H+zH_z(x,y,z) \end{pmatrix}, \tag{3.3}$$

where

$$F_x=\frac{\partial F}{\partial x}=-\frac{r_1}{K_1},\quad F_y=\frac{\partial F}{\partial y}=-\frac{a_1c_1}{(a_1+y)^2},\quad F_z=\frac{\partial F}{\partial z}=0,$$

$$G_x=\frac{\partial G}{\partial x}=\begin{cases}-\dfrac{a_2c_2}{(a_2+x)^2}, & \theta_1x+z<N-qK_2,\\ -\dfrac{\theta_1r_2qy}{(N-\theta_1x-z)^2}-\dfrac{a_2c_2}{(a_2+x)^2}, & \theta_1x+z>N-qK_2,\end{cases}$$

$$G_y=\frac{\partial G}{\partial y}=\begin{cases}-\dfrac{r_2}{K_2}+\dfrac{mz}{(b+y)^2}, & \theta_1x+z<N-qK_2,\\ -\dfrac{r_2q}{N-\theta_1x-z}+\dfrac{mz}{(b+y)^2}, & \theta_1x+z>N-qK_2,\end{cases}$$

$$G_z=\frac{\partial G}{\partial z}=\begin{cases}-\dfrac{m}{b+y}, & \theta_1x+z<N-qK_2,\\ -\dfrac{r_2qy}{(N-\theta_1x-z)^2}-\dfrac{m}{b+y}, & \theta_1x+z>N-qK_2,\end{cases}$$

$$H_x=\frac{\partial H}{\partial x}=\begin{cases}0, & \theta_1x+y+z<N,\\ -\dfrac{\theta_1em}{b+y}, & \theta_1x+y+z>N,\end{cases}$$

$$H_y=\frac{\partial H}{\partial y}=\begin{cases}\dfrac{bem}{(b+y)^2}, & \theta_1x+y+z<N,\\ -\dfrac{em(N-\theta_1x-z)}{(b+y)^2}, & \theta_1x+y+z>N,\end{cases}$$

$$H_z=\frac{\partial H}{\partial z}=\begin{cases}0, & \theta_1x+y+z<N,\\ -\dfrac{em}{b+y}, & \theta_1x+y+z>N.\end{cases}$$

(3.1) can possibly admit the following steady states:

$$E_0(0,0,0),\quad E_x\left(\frac{(r_1-d_1)K_1}{r_1},0,0\right),\quad E_y\left(0,\frac{(r_2-d_2)k}{r_2},0\right),\quad E_{xy}(x_1,y_1,0),\quad E_{yz}(0,y_2,z_2),$$

where x_1 and y_1 satisfy

$$\begin{cases}F_1(x,y)\triangleq r_1\left(1-\dfrac{x}{K_1}\right)-\dfrac{c_1y}{a_1+y}-d_1=0,\\ G_1(x,y)\triangleq r_2\left(1-\dfrac{y}{\min\left(K_2,(N-\theta_1x)/q\right)}\right)-\dfrac{c_2x}{a_2+x}-d_2=0,\end{cases}\tag{3.4}$$

y_2 and z_2 satisfy

$$\begin{cases} G_2(y,z) \triangleq r_2\left(1-\dfrac{y}{\min\left(K_2,(N-z)/q\right)}\right)-\dfrac{mz}{b+y}-d_2=0, \\ H_2(y,z) \triangleq e\min\left(1,\dfrac{N-z}{y}\right)\dfrac{my}{b+y}-h-d_3=0. \end{cases} \tag{3.5}$$

Theorem 3.3. *If $r_1<d_1$ and $r_2<d_2$, then $E_0(0,0,0)$ is globally asymptotically stable, otherwise $E_0(0,0,0)$ is unstable.*

Proof. The extinction equilibrium E_0 always exists. The Jacobian matrix of (3.1) evaluated at E_0 is

$$J(E_0)=\begin{pmatrix} r_1-d_1 & 0 & 0 \\ 0 & r_2-d_2 & 0 \\ 0 & 0 & -h-d_3 \end{pmatrix}.$$

Obviously, if $r_1<d_1$ and $r_2<d_2$, then the eigenvalues of $J(E_0)$ are negative, i.e. E_0 is locally asymptotically stable.

If $r_1<d_1$, then

$$\begin{aligned} \frac{\mathrm{d}x}{\mathrm{d}t} &= r_1x\left(1-\frac{x}{K_1}\right)-\frac{c_1xy}{a_1+y}-d_1x \\ &\le (r_1-d_1)x-\frac{c_1xy}{a_1+y}<0. \end{aligned}$$

Thus, $\lim\limits_{t\to\infty}x(t)=0$. When $r_2<d_2$, we have

$$\begin{aligned} \frac{\mathrm{d}y}{\mathrm{d}t} &= r_2y\left(1-\frac{y}{\min\left(K_2,(N-\theta_1x-z)/q\right)}\right)-\frac{c_2xy}{a_2+x}-\frac{myz}{b+y}-d_2y \\ &\le (r_2-d_2)y-\frac{c_2xy}{a_2+x}-\frac{myz}{b+y}<0. \end{aligned}$$

Therefore, $\lim_{t\to\infty}y(t)=0$, i.e. for any $\epsilon>0$, there exists a $T>0$ such that $y(t)<\epsilon$ when $t>T$. Let $\epsilon=b(h+d)/(2em)$, then

$$\begin{aligned} \frac{\mathrm{d}z}{\mathrm{d}t} &= e\min\left(1,\frac{N-\theta_1x-z}{y}\right)\frac{myz}{b+y}-hz-d_3z \\ &\le \frac{emyz}{b+y}-hz-d_3z \\ &\le z\left(\frac{em\epsilon}{b}-h-d_3\right)=-\frac{h+d_3}{2}z<0. \end{aligned}$$

Consequently, $\lim\limits_{t\to\infty}z(t)=0$. E_0 is globally asymptotically stable, otherwise E_0 is unstable. The proof is complete. $\square$

Theorem 3.4. *If* $r_1 > d_1$*, then* $E_x((r_1-d_1)K_1/r_1,0,0)$ *exists. Furthermore,*

(i) If

$$r_2 < d_2 + \frac{c_2K_1(r_1-d_1)}{r_1a_2+(r_1-d_1)K_1}, \tag{3.6}$$

then E_x *is locally asymptotically stable.*

(ii) If $r_2 < d_2$*, then* E_x *is globally asymptotically stable.*

Proof. (1) When $K_1 > Nr_1/[\theta_1(r_1-d_1)]$, from (3.3), the Jacobian matrix of (3.1) at E_x is given by

$$J(E_x)=\begin{pmatrix} -(r_1-d_1) & -\dfrac{c_1K_1(r_1-d_1)}{a_1r_1} & 0 \\ 0 & r_2-d_2-\dfrac{c_2K_1(r_1-d_1)}{r_1a_2+(r_1-d_1)K_1} & 0 \\ 0 & 0 & e\left(N-\theta_1\dfrac{(r_1-d_1)K_1}{r_1}\right)-h-d_3 \end{pmatrix}.$$

If $r_1 > d_1$ and (3.6) hold, then the eigenvalues of $J(E_x)$ are all negative, hence E_x is locally asymptotically stable.

(2) When $K_1 < Nr_1/[\theta_1(r_1-d_1)]$, from (3.3), the Jacobian matrix of (3.1) at E_x is

$$J(E_x)=\begin{pmatrix} -(r_1-d_1) & -\dfrac{c_1K_1(r_1-d_1)}{a_1r_1} & 0 \\ 0 & r_2-d_2-\dfrac{c_2K_1(r_1-d_1)}{r_1a_2+(r_1-d_1)K_1} & 0 \\ 0 & 0 & -h-d_3 \end{pmatrix}.$$

If $r_1 > d_1$ and (3.6) hold, then the eigenvalues of $J(E_x)$ are all negative, hence E_x is locally asymptotically stable.

From (3.1), it follows that if $r_2 < d_2$, then

$$\begin{aligned}\frac{\mathrm{d}y}{\mathrm{d}t}&=r_2y\left(1-\frac{y}{\min\left(K_2,(N-\theta_1x-z)/q\right)}\right)-\frac{c_2xy}{a_2+x}-\frac{myz}{b+y}-d_2y\\ &\le (r_2-d_2)y-\frac{c_2xy}{a_2+x}-\frac{myz}{b+y}<0.\end{aligned}$$

It is not difficult to deduce that $\lim_{t\to\infty}y(t)=0$, and thus $\lim_{t\to\infty}z(t)=0$. According to the theory of asymptotically autonomous systems [33], (3.1) reduces to a one-dimensional limit system

$$\frac{\mathrm{d}x}{\mathrm{d}t}=r_1x\left(1-\frac{x}{K_1}\right)-d_1x.$$

Then, $\lim_{t\to\infty}x(t)=(r_1-d_1)K_1/r_1$, which means that E_x is globally attractive and hence is globally asymptotically stable. □

Theorem 3.5. *If* $r_2>d_2$, *then* $E_y(0,(r_2-d_2)k/r_2,0)$ *exists. In addition,*

(i) If

$$r_1<d_1+\frac{c_1k(r_2-d_2)}{r_2a_1+(r_2-d_2)k}, \tag{3.7}$$

$$h+d_3>\max\left\{\frac{em(r_2-d_2)k}{r_2b+(r_2-d_2)k},\frac{emr_2N}{r_2b+(r_2-d_2)k}\right\}, \tag{3.8}$$

then E_y *is locally asymptotically stable.*

(ii) If $r_1<d_1$, *then* E_y *is globally asymptotically stable.*

Proof. (1) When $N/q<\min\{K_2,Nr_2/(r_2-d_2)\},k=N/q$. By (3.3), the Jacobian matrix of (3.1) at E_y is

$$J(E_y)=\begin{pmatrix} r_1-d_1-\dfrac{c_1N(r_2-d_2)}{r_2qa_1+(r_2-d_2)N} & 0 & 0 \\ -\dfrac{\theta_1a_2(r_2-d_2)^2+c_2N(r_2-d_2)}{a_2r_2q} & -(r_2-d_2) & -\dfrac{(r_2-d_2)^2}{r_2q}-\dfrac{mN(r_2-d_2)}{r_2qb+(r_2-d_2)N} \\ 0 & 0 & \dfrac{emN(r_2-d_2)}{r_2qb+(r_2-d_2)N}-h-d_3 \end{pmatrix}.$$

If $r_2>d_2$ and

$$r_1<d_1+\frac{c_1(r_2-d_2)N/q}{r_2a_1+(r_2-d_2)N/q},\quad h+d_3>\frac{em(r_2-d_2)N/q}{r_2b+(r_2-d_2)N/q},$$

then the eigenvalues of $J(E_y)$ are all negative, hence E_y is locally asymptotically stable.

(2) When $K_2>N/q>Nr_2/(r_2-d_2),k=N/q$. By (3.3), the Jacobian matrix of (3.1) at E_y is

$$J(E_y)=\begin{pmatrix} r_1-d_1-\dfrac{c_1N(r_2-d_2)}{r_2qa_1+(r_2-d_2)N} & 0 & 0 \\ -\dfrac{\theta_1a_2(r_2-d_2)^2+c_2N(r_2-d_2)}{a_2r_2q} & -(r_2-d_2) & -\dfrac{(r_2-d_2)^2}{r_2q}-\dfrac{mN(r_2-d_2)}{r_2qb+(r_2-d_2)N} \\ 0 & 0 & \dfrac{emNr_2q}{r_2qb+(r_2-d_2)N}-h-d_3 \end{pmatrix}.$$

If $r_2>d_2$ and

$$r_1<d_1+\frac{c_1(r_2-d_2)N/q}{r_2a_1+(r_2-d_2)N/q},\quad h+d_3>\frac{emr_2N}{r_2b+(r_2-d_2)N/q},$$

then the eigenvalues of $J(E_y)$ are all negative, hence E_y is locally asymptotically stable.

(3) When $K_2 < \min\{N/q, Nr_2/(r_2-d_2)\}, k=K_2$. By (3.3), the Jacobian matrix of (3.1) at E_y is

$$J(E_y)=\begin{pmatrix} r_1-d_1-\dfrac{c_1K_2(r_2-d_2)}{r_2a_1+(r_2-d_2)K_2} & 0 & 0 \\ -\dfrac{c_2K_2(r_2-d_2)}{a_2r_2} & -(r_2-d_2) & -\dfrac{mr_2}{r_2b+(r_2-d_2)K_2} \\ 0 & 0 & \dfrac{emK_2(r_2-d_2)}{r_2b+(r_2-d_2)K_2}-h-d_3 \end{pmatrix}.$$

If $r_2 > d_2$ and

$$r_1 < d_1+\frac{c_1K_2(r_2-d_2)}{r_2a_1+(r_2-d_2)K_2}, \quad h+d_3 > \frac{em(r_2-d_2)K_2}{r_2b+(r_2-d_2)K_2},$$

then the eigenvalues of $J(E_y)$ are all negative, hence E_y is locally asymptotically stable.

(4) When $Nr_2/(r_2-d_2) < K_2 < N/q, k=K_2$. By (3.3), the Jacobian matrix of (3.1) at E_y is

$$J(E_y)=\begin{pmatrix} r_1-d_1-\dfrac{c_1K_2(r_2-d_2)}{r_2a_1+(r_2-d_2)K_2} & 0 & 0 \\ -\dfrac{c_2K_2(r_2-d_2)}{a_2r_2} & -(r_2-d_2) & -\dfrac{mr_2}{r_2b+(r_2-d_2)K_2} \\ 0 & 0 & \dfrac{emNr_2}{r_2b+(r_2-d_2)K_2}-h-d_3 \end{pmatrix}.$$

If $r_2 > d_2$ and

$$r_1 < d_1+\frac{c_1K_2(r_2-d_2)}{r_2a_1+(r_2-d_2)K_2}, \quad h+d_3 > \frac{emr_2N}{r_2b+(r_2-d_2)K_2},$$

then the eigenvalues of $J(E_y)$ are all negative, hence E_y is locally asymptotically stable.

Thus, if $r_2 > d_2$ and (3.7) and (3.8) hold, then E_y is locally asymptotically stable. Furthermore, from

$$\begin{aligned}\frac{\mathrm{d}y}{\mathrm{d}t} &= r_2y\left(1-\frac{y}{\min\left(K_2,(N-\theta_1x-z)/q\right)}\right)-\frac{c_2xy}{a_2+x}-\frac{myz}{b+y}-d_2y \\ &\le y\left(r_2-d_2-\frac{r_2y}{k}\right),\end{aligned}$$

by the comparison theorem, it follows that $\limsup_{t\to\infty} y(t) \le (r_2-d_2)k/r_2$. That is, for any $\epsilon > 0$, there exists a $T > 0$ such that $y(t) < (r_2-d_2)k/r_2+\epsilon$ for $t > T$. Taking

$$\epsilon = \frac{1}{2}\left(\frac{h+d_3}{em}-\frac{(r_2-d_2)k}{r_2b+(r_2-d_2)k}\right).$$

If (3.8) is satisfied, then

$$\begin{aligned}\frac{\mathrm{d}z}{\mathrm{d}t}&=e\min\left(1,\frac{N-\theta_1x-z}{y}\right)\frac{myz}{b+y}-hz-d_3z\\&\le z\left(\frac{emy}{b+y}-h-d_3\right)\\&<z\left(\frac{em(r_2-d_2)k}{r_2b+(r_2-d_2)k}-h-d_3+em\epsilon\right)\\&=\frac{z}{2}\left(\frac{em(r_2-d_2)k}{r_2b+(r_2-d_2)k}-h-d_3\right)<0.\end{aligned}$$

Thus, $\lim_{t\to\infty}z(t)=0$. Since $r_1<d_1$, one has $\lim_{t\to\infty}x(t)=0$. According to the theory of asymptotically autonomous systems [33], (3.1) reduces to the limit system

$$\frac{\mathrm{d}y}{\mathrm{d}t}=y\left(r_2-d_2-\frac{r_2y}{k}\right).$$

It is easy to deduce that $\lim\limits_{t\to\infty}y(t)=(r_2-d_2)k/r_2$, which implies that E_y is globally attractive and thus globally asymptotically stable. □

When the predator species does not exist, i.e. $z=0$, (3.1) simplifies to the following system:

$$\begin{cases}\dfrac{\mathrm{d}x}{\mathrm{d}t}=r_1x\left(1-\dfrac{x}{K_1}\right)-\dfrac{c_1xy}{a_1+y}-d_1x\triangleq xF_1(x,y),\\[2ex]\dfrac{\mathrm{d}y}{\mathrm{d}t}=r_2y\left(1-\dfrac{y}{\min\left(K_2,(N-\theta_1x)/q\right)}\right)-\dfrac{c_2xy}{a_2+x}-d_2y\triangleq yG_1(x,y),\end{cases}\tag{3.9}$$

where

$$\begin{aligned}F_1(x,y)&=r_1\left(1-\frac{x}{K_1}\right)-\frac{c_1y}{a_1+y}-d_1,\\G_1(x,y)&=r_2\left(1-\frac{y}{\min\left(K_2,(N-\theta_1x)/q\right)}\right)-\frac{c_2x}{a_2+x}-d_2.\end{aligned}$$

Moreover, the invariant set of (3.9) is $\Omega=\{(x,y):0<x<K_1,0<y<k\}$.

The following discussion explores (3.9) in the region Ω to analyze the existence of non-periodic solutions. It is noted that the vector field defined by (3.9) satisfies local Lipschitz continuity, which guarantees the existence and uniqueness of solutions to (3.9). Furthermore, the vector field is C^1, which implies that the classical Dulac criterion is not applicable. Thus, the Dulac criterion is undefined in this scenario [24,40].

Lemma 3.1. *Consider a locally Lipschitz system*

$$\frac{\mathrm{d}x}{\mathrm{d}t}=f(x),\quad x\in\Phi\subset\mathbb{R}^2.\tag{3.10}$$

If Φ *is an open bounded set in* $\mathbb{R}^2$, *and there exists a continuous function* $D:\Phi\to\mathbb{R}$ *and a constant* $\alpha>0$ *such that*

$$\operatorname{div}\big(\chi(x)f(x)\big)\le-\alpha \quad \textit{a.e. in } D,$$

then (3.10) *has no non-trivial periodic orbits within* Φ. *Moreover, all solutions within* Φ *will eventually approach equilibrium, excluding solutions that form closed orbits. The existence of non-trivial periodic orbits would imply inconsistency with the condition on* div.

Theorem 3.6. *System* (3.9) *has no non-trivial periodic solutions within* Ω.

Proof. Let $\chi(x,y)=1/(xy)$, then it is a C^1 function in Ω and

$$\begin{aligned}
&\frac{1}{xy}xF_1(x,y)=\frac{r_1-d_1}{y}-\frac{r_1x}{K_1y}-\frac{c_1}{a_1+y},\\
&\frac{1}{xy}yG_1(x,y)=\begin{cases} lc\dfrac{r_2-d_2}{x}-\dfrac{r_2y}{K_2x}-\dfrac{c_2}{a_2+x}, & \theta_1x<N-qK_2,\\ \dfrac{r_2-d_2}{x}-\dfrac{r_2qy}{x(N-\theta_1x)}-\dfrac{c_2}{a_2+x}, & \theta_1x>N-qK_2.\end{cases}
\end{aligned}$$

One onely discusses the case when $K_2\le N/q$. The case when $K_2>N/q$ can be proved similarly. The following discussion is divided into two cases.

- In $\Omega_{12}\subset\Omega$, where $\theta_1x<N-qK_2$, one gets

$$\begin{aligned}
\operatorname{div}\big(\chi(x,y)f(x,y)\big)&=\frac{\partial}{\partial x}\left(\frac{r_1-d_1}{y}-\frac{r_1x}{K_1y}-\frac{c_1}{a_1+y}\right)+\frac{\partial}{\partial y}\left(\frac{r_2-d_2}{x}-\frac{r_2qy}{x(N-\theta_1x)}-\frac{c_2}{a_2+x}\right)\\
&=-\frac{r_1}{K_1y}-\frac{r_2q}{x(N-\theta_1x)}\le-\alpha_1.
\end{aligned}$$

- In $\Omega_{34}\subset\Omega$, where $\theta_1x>N-qK_2$, one obtains

$$\begin{aligned}
\operatorname{div}\big(\chi(x,y)f(x,y)\big)&=\frac{\partial}{\partial x}\left(\frac{r_1-d_1}{y}-\frac{r_1x}{K_1y}-\frac{c_1}{a_1+y}\right)+\frac{\partial}{\partial y}\left(\frac{r_2-d_2}{x}-\frac{r_2y}{K_2x}-\frac{c_2}{a_2+x}\right)\\
&=-\frac{r_1}{K_1y}-\frac{r_2}{K_2x}\le-\alpha_2.
\end{aligned}$$

Let $\alpha=\min\{\alpha_1,\alpha_2\}$, where

$$\alpha_1=\min_{(x,y)\in\Omega_{12}}\left(\frac{r_1}{K_1y}+\frac{r_2q}{x(N-\theta_1x)}\right),\quad \alpha_2=\min_{(x,y)\in\Omega_{34}}\left(\frac{r_1}{K_1y}+\frac{r_2}{K_2x}\right).$$

Clearly, $\alpha>0$. By Lemma 3.1, (3.9) has no non-trivial periodic solutions in Ω. ☐

The region Δ^* is divided into several subregions according to the different cases of the minimum function.

(i) When $K_2 > N/q$,

$$\Delta_1 = \{(x,y,z) \in \Delta^* : \theta_1 x + z > N - qK_2, \theta_1 x + y + z < N\},$$
$$\Delta_2 = \{(x,y,z) \in \Delta^* : \theta_1 x + z > N - qK_2, \theta_1 x + y + z > N\}.$$

(ii) When $K_2 \le N/q$,

$$\Delta_1 = \{(x,y,z) \in \Delta^* : \theta_1 x + z > N - qK_2, \theta_1 x + y + z < N\},$$
$$\Delta_2 = \{(x,y,z) \in \Delta^* : \theta_1 x + z > N - qK_2, \theta_1 x + y + z > N\},$$
$$\Delta_3 = \{(x,y,z) \in \Delta^* : \theta_1 x + z < N - qK_2, \theta_1 x + y + z < N\},$$
$$\Delta_4 = \{(x,y,z) \in \Delta^* : \theta_1 x + z < N - qK_2, \theta_1 x + y + z > N\}.$$

Theorem 3.7. *If $r_1 > d_1, r_2 > d_2, K_1 > \max\{S_1, S_3\}, k > S_2$, then $E_{xy}(x_1, y_1, 0)$ exists, where S_i $(i = 1,2,3)$ is defined by* (3.17) *and* (3.19). *Furthermore,*

(i) if

$$h + d_3 > \max\left\{\frac{emy_1}{b + y_1}, \frac{em(N - \theta_1 x_1)}{b + y_1}\right\}, \tag{3.11}$$

$$J_{11}^{(k)} J_{22}^{(k)} > J_{12}^{(k)} J_{21}^{(k)} \quad (k = 1,3), \tag{3.12}$$

then E_{xy} is locally asymptotically stable, where $J_{ij}^{(k)}$ represents the (i,j)-th element of $J^{(k)}(E_{xy})$ $(i,j = 1,2)$;

(ii) if

$$h + d_3 > me, \tag{3.13}$$

$$r_2 > d_2 + \frac{c_2 K_1 (r_1 - d_1)}{r_1 a_2 + (r_1 - d_1) K_1}, \tag{3.14}$$

$$r_1 > d_1 + \frac{c_1 k (r_2 - d_2)}{r_2 a_1 + (r_2 - d_2) k}, \tag{3.15}$$

then E_{xy} is globally asymptotically stable.

Proof. First, the existence of E_{xy} is verified. The discussion is divided into two cases.

(1) When $K_2 > N/q$,

$$G_1(x,y) = r_2\left(1 - \frac{y}{(N - \theta_1 x)/q}\right) - \frac{c_2 x}{a_2 + x} - d_2.$$

Since x and y satisfy the solution of Eq. (3.4), (x_1, y_1) is the intersection of the following two curves:

$$y = \frac{(r_2 - d_2)(N - \theta_1 x)}{r_2 q} - \frac{c_2 x (N - \theta_1 x)}{a_2 + x}, \quad y = \frac{a_1 (r_1 - r_1 x/K_1 - d_1)}{c_1 - (r_1 - r_1 x/K_1 - d_1)}.$$

Let
$$U(x)=\left(\frac{r_2-d_2}{r_2q}-\frac{c_2x}{a_2+x}\right)(N-\theta_1x)-\frac{a_1(r_1-r_1x/K_1-d_1)}{c_1-(r_1-r_1x/K_1-d_1)}. \tag{3.16}$$
When $r_1>d_1, K_1>S_1, N/q>S_2$, it follows from (3.16) that

$$U\left(\frac{(r_1-d_1)K_1}{r_1}\right)<0, \quad U(0)>0,$$

where
$$S_1=\frac{a_2r_1(r_2-d_2)}{(r_1-d_1)[r_2qc_2-(r_2-d_2)]}, \quad S_2=\frac{a_1r_2(r_1-d_1)}{(r_2-d_2)[c_1-(r_1-d_1)]}. \tag{3.17}$$
By the intermediate value theorem, there exists a unique $x_1\in(0,(r_1-d_1)K_1/r_1)$ such that $U(x_1)=0$. Additionally, when $x_1>\max\{0,(r_1-d_1-c_1)K_1/r_1\}$, one has

$$y_1=\frac{a_1(r_1-r_1x_1/K_1-d_1)}{c_1-(r_1-r_1x_1/K_1-d_1)}>0.$$

Thus, E_{xy} exists uniquely.

(2) When $K_2\le N/q$,

$$G_1(x,y)=\begin{cases} r_2\left(1-\dfrac{y}{K_2}\right)-\dfrac{c_2x}{a_2+x}-d_2, & \theta_1x<N-qK_2, \\ r_2\left(1-\dfrac{y}{(N-\theta_1x)/q}\right)-\dfrac{c_2x}{a_2+x}-d_2, & \theta_1x>N-qK_2. \end{cases}$$

If $\theta_1x>N-qK_2$, then the discussion on the existence of (x_1,y_1) follows the same scenario as in case (1). For $\theta_1x\le N-qK_2$, one has

$$G_1(x,y)=r_2\left(1-\frac{y}{K_2}\right)-\frac{c_2x}{a_2+x}-d_2.$$

Since x_1 and y_1 are solutions of (3.4), (x_1,y_1) is the intersection of the following two curves:
$$x=\frac{K_1}{r_1}\left(r_1-d_1-\frac{c_1y}{a_1+y}\right), \quad x=\frac{a_2(r_2-r_2y/K_2-d_2)}{c_2-(r_2-r_2y/K_2-d_2)}.$$
Let
$$V(y)=\frac{K_1}{r_1}(r_1-d_1-c_1y/a_1+y)-\frac{a_2(r_2-r_2y/K_2-d_2)}{c_2-(r_2-r_2y/K_2-d_2)}. \tag{3.18}$$
When $r_2>d_2, K_2>S_2, K_1>S_3$, it follows from (3.18) that

$$V\left(\frac{(r_2-d_2)K_2}{r_2}\right)<0, \quad V(0)>0,$$

where

$$S_3=\frac{a_2r_1(r_2-d_2)}{(r_1-d_1)[c_2-(r_2-d_2)]}. \tag{3.19}$$

By the intermediate value theorem, there exists a unique $y_1\in(0,(r_2-d_2)K_2/r_2)$ such that $V(y_1)=0$. Additionally, when $y_1>\max\{0,(r_2-d_2)K_2/r_2\}$, one has

$$x_1=\frac{a_2(r_2-r_2y_1/K_2-d_2)}{c_2-(r_2-r_2y_1/K_2-d_2)}>0,$$

Thus, E_{xy} exists uniquely.

In summary, if $r_1>d_1,r_2>d_2,K_1>\max\{S_1,S_3\},k>S_2$, then E_{xy} exists. To prove the stability of E_{xy}, one only discusses the case when $K_2\leq N/q$. The case when $K_2>N/q$ can be proved similarly. The discussion is divided into two cases.

(1) If E_{xy} is in the region

$$\Delta_1=\{(x,y,z)\in\Delta^*:\theta_1x+z>N-qK_2,\theta_1x+y+z<N\},$$

then $\theta_1x_1>N-qK_2,\ \theta_1x_1+y_1<N$. By (3.3), the Jacobian matrix of (3.1) at E_{xy} is

$$J^{(1)}(E_{xy})=\begin{pmatrix}-\frac{r_1x_1}{K_1} & -\frac{a_1c_1x_1}{(a_1+y_1)^2} & 0\\ -d\frac{r_2\theta_1qy_1^2}{(N-\theta_1x_1)^2}-\frac{a_2c_2y_1}{(a_2+x_1)^2} & -\frac{qr_2y_1}{N-\theta_1x_1} & -\frac{r_2qy_1^2}{(N-\theta_1x_1)^2}-\frac{my_1}{b+y_1}\\ 0 & 0 & \frac{emy_1}{b+y_1}-h-d_3\end{pmatrix}.$$

The characteristic equation is

$$\left[\lambda-\left(\frac{emy_1}{b+y_1}-h-d_3\right)\right]\left[\lambda^2-(J_{11}^{(1)}+J_{22}^{(1)})\lambda+J_{11}^{(1)}J_{22}^{(1)}-J_{12}^{(1)}J_{21}^{(1)}\right]=0,$$

where $J_{ij}^{(1)}$ refers to the element in the i-th row and j-th column of $J^{(1)}(E_{xy})$ (i,j=1,2), and

$$\begin{aligned}&J_{11}^{(1)}+J_{22}^{(1)}=-\left(\frac{r_1x_1}{K_1}+\frac{qr_2y_1}{N-\theta_1x_1}\right),\\&J_{11}^{(1)}J_{22}^{(1)}-J_{12}^{(1)}J_{21}^{(1)}=x_1y_1\frac{r_1qr_2}{K_1(N-\theta_1x_1)}-x_1y_1\frac{a_1c_1}{(a_1+y_1)^2}\left(\frac{r_2\theta_1qy_1}{(N-\theta_1x_1)^2}+\frac{a_2c_2}{(a_2+x_1)^2}\right).\end{aligned}$$

Thus, when

$$h+d_3>\frac{emy_1}{b+y_1}, \tag{3.20}$$

$$J_{11}^{(1)}J_{22}^{(1)}>J_{12}^{(1)}J_{21}^{(1)}, \tag{3.21}$$

the eigenvalues of $J^{(1)}(E_{xy})$ all have negative real parts, and E_{xy} is locally asymptotically stable.

To prove the global stability of E_{xy}, when $e<(h+d_3)/m$, one has

$$\frac{\mathrm{d}z}{\mathrm{d}t}=e\min\left(1,\frac{N-\theta_1x-z}{y}\right)\frac{myz}{b+y}-hz-d_3z\leq z(em-h-d_3)<0.$$

Thus, $\lim_{t\to\infty}z(t)=0$. According to the theory of asymptotically autonomous systems [33], (3.1) reduces to the planar system (3.9), which has four equilibria $(0,0)$, $((r_1-d_1)K_1/r_1,0)$, $(0,(r_2-d_2)k/r_2)$, and (x_1,y_1). It is trivial to verify that $(0,0)$ is a unstable node. When

$$r_2>d_2+\frac{c_2K_1(r_1-d_1)}{r_1a_2+(r_1-d_1)K_1},$$

$((r_1-d_1)K_1/r_1,0)$ is a saddle point. When

$$r_1>d_1+\frac{c_1k(r_2-d_2)}{r_2a_1+(r_2-d_2)k},$$

$(0,(r_2-d_2)k/r_2)$ is a saddle point. When (3.21) holds, (x_1,y_1) is locally asymptotically stable. Since Ω is compact and positively invariant, system (3.9) cannot have closed orbits. By the Poincaré-Bendixson theorem, all trajectories in Ω eventually converge to (x_1,y_1), i.e. E_{xy} is globally stable. This demonstrates that (3.9) is globally asymptotically stable within Δ^*, with E_{xy} being locally asymptotically stable [33].

(2) If E_{xy} is in the region

$$\Delta_2=\{(x,y,z)\in\Delta^*:\theta_1x+z>N-qK_2,\theta_1x+y+z>N\},$$

then $\theta_1x_1>N-qK_2$ and $\theta_1x_1+y_1>N$. From (3.3), the Jacobian matrix of (3.1) at E_{xy} is

$$J^{(2)}(E_{xy})=\begin{pmatrix} -\dfrac{r_1x_1}{K_1} & -\dfrac{a_1c_1x_1}{(a_1+y_1)^2} & 0 \\ -\dfrac{r_2\theta_1qy_1^2}{(N-\theta_1x_1)^2}-\dfrac{a_2c_2y_1}{(a_2+x_1)^2} & -\dfrac{qr_2y_1}{N-\theta_1x_1} & -\dfrac{r_2qy_1^2}{(N-\theta_1x_1)^2}-\dfrac{my_1}{b+y_1} \\ 0 & 0 & \dfrac{em(N-\theta_1x_1)}{b+y_1}-h-d_3 \end{pmatrix}.$$

The characteristic equation reads

$$\left[\lambda-\left(\frac{em(N-\theta_1x_1)}{b+y_1}-h-d_3\right)\right]\left[\lambda^2-(J_{11}^{(2)}+J_{22}^{(2)})\lambda+J_{11}^{(2)}J_{22}^{(2)}-J_{12}^{(2)}J_{21}^{(2)}\right]=0,$$

where $J_{ij}^{(2)}$ refers to the (i,j)-th element of $J^{(2)}(E_{xy})$, and it can be seen that $J_{ij}^{(1)}=J_{ij}^{(2)}$ $(i,j=1,2)$.

When

$$h+d_3>\frac{em(N-\theta_1x_1)}{b+y_1},\quad J_{11}^{(1)}J_{22}^{(1)}>J_{12}^{(1)}J_{21}^{(1)},$$

the eigenvalues of $J^{(2)}(E_{xy})$ have negative real parts, and E_{xy} is locally asymptotically stable. Similarly, it can be proven that, when (3.13)-(3.15) are satisfied, E_{xy} is globally asymptotically stable in Δ_2.

(3) If E_{xy} is in the region

$$\Delta_3=\{(x,y,z)\in\Delta^*:\theta_1x+z<N-qK_2,\theta_1x+y+z<N\},$$

then $\theta_1x_1<N-qK_2,\theta_1x_1+y_1<N$. From (3.3), it follows that

$$J^{(3)}(E_{xy})=\begin{pmatrix} -\dfrac{r_1x_1}{K_1} & -\dfrac{a_1c_1x_1}{(a_1+y_1)^2} & 0 \\ -\dfrac{a_2c_2y_1}{(a_2+x_1)^2} & -\dfrac{r_2y_1}{K_2} & -\dfrac{my_1}{b+y_1} \\ 0 & 0 & \dfrac{emy_1}{b+y_1}-h-d_3 \end{pmatrix},$$

and the characteristic equation is

$$\left[\lambda-\left(\frac{emy_1}{b+y_1}-h-d_3\right)\right]\left[\lambda^2-(J_{11}^{(3)}+J_{22}^{(3)})\lambda+J_{11}^{(3)}J_{22}^{(3)}-J_{12}^{(3)}J_{21}^{(3)}\right]=0,$$

where $J_{ij}^{(3)}$ refers to the (i,j)-th element of $J^{(3)}(E_{xy})$, and

$$\begin{aligned} &J_{11}^{(3)}+J_{22}^{(3)}=-\left(\frac{r_1x_1}{K_1}+\frac{r_2y_1}{K_2}\right), \\ &J_{11}^{(3)}J_{22}^{(3)}-J_{12}^{(3)}J_{21}^{(3)}=x_1y_1\frac{r_1r_2}{K_2K_1}-x_1y_1\frac{a_1c_1a_2c_2}{(a_1+y_1)^2(a_2+x_1)^2}. \end{aligned}$$

When

$$h+d_3>\frac{emy_1}{b+y_1},\quad J_{11}^{(3)}J_{22}^{(3)}>J_{12}^{(3)}J_{21}^{(3)},$$

the eigenvalues of $J^{(3)}(E_{xy})$ have negative real parts, and E_{xy} is locally asymptotically stable. Similarly, it can be proven that, when (3.13)-(3.15) are satisfied, E_{xy} is globally asymptotically stable in Δ_3.

(4) If E_{xy} is in the region

$$\Delta_4=\{(x,y,z)\in\Delta^*:\theta_1x+z<N-qK_2,\theta_1x+y+z>N\},$$

then $\theta_1x_1<N-qK_2$ and $\theta_1x_1+y_1>N$. By (3.3), the Jacobian matrix of (3.1) at E_{xy} is

$$J^{(4)}(E_{xy})=\begin{pmatrix} -\dfrac{r_1x_1}{K_1} & -\dfrac{a_1c_1x_1}{(a_1+y_1)^2} & 0 \\ -\dfrac{a_2c_2y_1}{(a_2+x_1)^2} & -\dfrac{r_2y_1}{K_2} & -\dfrac{my_1}{b+y_1} \\ 0 & 0 & \dfrac{em(N-\theta_1x_1)}{b+y_1}-h-d_3 \end{pmatrix}.$$

The characteristic equation is

$$\left[\lambda-\left(\frac{em(N-\theta_1x_1)}{b+y_1}-h-d_3\right)\right]\left[\lambda^2-(J_{11}^{(4)}+J_{22}^{(4)})\lambda+J_{11}^{(4)}J_{22}^{(4)}-J_{12}^{(4)}J_{21}^{(4)}\right]=0,$$

where $J_{ij}^{(4)}$ refers to the (i,j)-th element of $J^{(4)}(E_{xy})$, and it can be seen that $J_{ij}^{(1)}=J_{ij}^{(4)}$ $(i,j=1,2)$. When

$$h+d_3>\frac{em(N-\theta_1x_1)}{b+y_1},\quad J_{11}^{(3)}J_{22}^{(3)}>J_{12}^{(3)}J_{21}^{(3)},$$

the eigenvalues of $J^{(4)}(E_{xy})$ have negative real parts, and E_{xy} is locally asymptotically stable.

Similarly, it can be proven that, when (3.13)-(3.15) are satisfied, E_{xy} is globally asymptotically stable within Δ_4. □

When prey does not exist, i.e. $x=0$, (3.1) simplifies to the following form:

$$\begin{cases}\dfrac{\mathrm{d}y}{\mathrm{d}t}=r_2y\left(1-\dfrac{y}{\min(K_2,(N-z)/q)}\right)-\dfrac{myz}{b+y}-d_2y\triangleq yG_2(y,z),\\[2mm] \dfrac{\mathrm{d}z}{\mathrm{d}t}=e\min\left(1,\dfrac{N-z}{y}\right)\dfrac{myz}{b+y}-hz-d_3z\triangleq zH_2(y,z).\end{cases}\tag{3.22}$$

According to the results of [53], it can be concluded that (3.22) has an interior equilibrium point. Therefore, (3.1) has a boundary equilibrium point in the form of $E_{yz}(0,y_2,z_2)$.

Theorem 3.8. *If*

$$\begin{aligned}&J_{22}^{(k)}+J_{33}^{(k)}<0 && (k=1,\ldots,4),\\ &r_1<d_1+\frac{c_1y_2}{a_1+y_2},\quad J_{22}^{(l)}J_{33}^{(l)}>J_{23}^{(l)}J_{32}^{(l)} && (l=2,4),\end{aligned}\tag{3.23}$$

then $E_{yz}(0,y_2,z_2)$ is locally asymptotically stable.

Proof. For the stability of E_{yz} in (3.1), it only needs to discuss the case when $K_2\le N/q$. The case when $K_2>N/q$ can be proven similarly. The discussion is divided into the following four cases.

(1) If E_{yz} is in the region

$$\Delta_1=\{(x,y,z)\in\Delta^*:\theta_1x+z>N-qK_2,\theta_1x+y+z<N\},$$

then $z_2>N-qK_2,y_2+z_2<N$. By (3.3), the Jacobian matrix of (3.1) at E_{yz} is

$$J^{(1)}(E_{yz})=\begin{pmatrix} r_1-d_1-\dfrac{c_1y_2}{a_1+y_2} & 0 & 0\\ -\dfrac{r_2\theta_1qy_2^2}{(N-z_2)^2}-\dfrac{c_2y_2}{a_2} & -\dfrac{qr_2y_2}{N-z_2}+\dfrac{mz_2y_2}{(b+y_2)^2} & -\dfrac{r_2qy_2^2}{(N-z_2)^2}-\dfrac{my_2}{b+y_2}\\ 0 & \dfrac{bemz_2}{(b+y_2)^2} & 0\end{pmatrix}.$$

The characteristic equation is

$$\left[\lambda-\left(r_1-d_1-\frac{c_1y_2}{a_1+y_2}\right)\right]\left[\lambda^2-\left(J_{22}^{(1)}+J_{33}^{(1)}\right)\lambda+J_{22}^{(1)}J_{33}^{(1)}-J_{23}^{(1)}J_{32}^{(1)}\right]=0,$$

where $J_{ij}^{(1)}$ refers to the (i,j)-th element of $J^{(1)}(E_{yz})$ $(i,j=2,3)$, and

$$\begin{aligned}
J_{22}^{(1)}+J_{33}^{(1)}&=-\frac{qr_2y_2}{N-z_2}+\frac{mz_2y_2}{(b+y_2)^2},\\
J_{22}^{(1)}J_{33}^{(1)}-J_{23}^{(1)}J_{32}^{(1)}&=\frac{bemz_2}{(b+y_2)^2}\left[\frac{r_2qy_2^2}{(N-z_2)^2}+\frac{my_2}{b+y_2}\right].
\end{aligned}$$

Thus, when

$$r_1<d_1+\frac{c_1y_2}{a_1+y_2},\quad J_{22}^{(1)}+J_{33}^{(1)}<0,$$

the eigenvalues of $J^{(1)}(E_{yz})$ have negative real parts, and E_{yz} is locally asymptotically stable.

(2) If E_{yz} is in the region

$$\Delta_2=\{(x,y,z)\in\Delta^*:\theta_1x+z>N-qK_2,\theta_1x+y+z>N\},$$

then $z_2>N-qK_2$ and $y_2+z_2>N$. By (3.3), the Jacobian matrix of (3.1) at E_{yz} is

$$J^{(2)}(E_{yz})=\begin{pmatrix}
r_1-d_1-\dfrac{c_1y_2}{a_1+y_2} & 0 & 0\\
-\dfrac{r_2\theta_1qy_2^2}{(N-z_2)^2}-\dfrac{c_2y_2}{a_2} & -\dfrac{qr_2y_2}{N-z_2}+\frac{mz_2y_2}{(b+y_2)^2} & -\dfrac{r_2qy_2^2}{(N-z_2)^2}-\dfrac{my_2}{b+y_2}\\
-\dfrac{\theta_1emz_2}{b+y_2} & -\dfrac{em(N-z_2)z_2}{(b+y_2)^2} & -\dfrac{emz_2}{b+y_2}
\end{pmatrix}.$$

The characteristic equation is

$$\left[\lambda-\left(r_1-d_1-\frac{c_1y_2}{a_1+y_2}\right)\right]\left[\lambda^2-\left(J_{22}^{(2)}+J_{33}^{(2)}\right)\lambda+J_{22}^{(2)}J_{33}^{(2)}-J_{23}^{(2)}J_{32}^{(2)}\right]=0,$$

where $J_{ij}^{(2)}$ refers to the (i,j)-th element of $J^{(2)}(E_{yz})$ $(i,j=2,3)$, and

$$\begin{aligned}
&J_{22}^{(2)}+J_{33}^{(2)}=-\frac{qr_2y_2}{N-z_2}+\frac{mz_2y_2}{(b+y_2)^2}-\frac{emz_2}{b+y_2},\\
&J_{22}^{(2)}J_{33}^{(2)}-J_{23}^{(2)}J_{32}^{(2)}=-\frac{emz_2}{b+y_2}\left[\frac{mz_2y_2}{(b+y_2)^2}-\frac{qr_2y_2}{N-z_2}\right]+\frac{emz_2(N-z_2)}{(b+y_2)^2}\left[\frac{r_2qy_2^2}{(N-z_2)^2}+\frac{my_2}{b+y_2}\right].
\end{aligned}$$

Furthermore, when

$$r_1<d_1+\frac{c_1y_2}{a_1+y_2},\quad J_{22}^{(2)}+J_{33}^{(2)}<0,\quad J_{22}^{(2)}J_{33}^{(2)}>J_{23}^{(2)}J_{32}^{(2)},$$

the eigenvalues of $J^{(2)}(E_{yz})$ all have negative real parts, and E_{yz} is locally asymptotically stable.

(3) If E_{yz} is in the region

$$\Delta_3 = \{(x,y,z) \in \Delta^* : \theta_1 x + z < N - qK_2, \theta_1 x + y + z < N\},$$

then $z_2 < N - qK_2, y_2 + z_2 < N$. By (3.3), the Jacobian matrix of (3.1) at E_{yz} is

$$J^{(3)}(E_{yz}) = \begin{pmatrix} r_1 - d_1 - \dfrac{c_1 y_2}{a_1 + y_2} & 0 & 0 \\ -\dfrac{c_2 y_2}{a_2} & -\dfrac{r_2 y_2}{K_2} + \dfrac{m z_2 y_2}{(b+y_2)^2} & -\dfrac{m y_2}{b + y_2} \\ 0 & \dfrac{bemz_2}{(b+y_2)^2} & 0 \end{pmatrix}.$$

The characteristic equation is

$$\left[\lambda - \left(r_1 - d_1 - \frac{c_1 y_2}{a_1 + y_2}\right)\right]\left[\lambda^2 - (J_{22}^{(3)} + J_{33}^{(3)})\lambda + J_{22}^{(3)} J_{33}^{(3)} - J_{23}^{(3)} J_{32}^{(3)}\right] = 0,$$

where $J_{ij}^{(3)}$ refers to the (i,j)-th element of $J^{(3)}(E_{yz})$ $(i,j = 2,3)$, and

$$J_{22}^{(3)} + J_{33}^{(3)} = -\frac{r_2 y_2}{K_2} + \frac{m z_2 y_2}{(b+y_2)^2}, \quad J_{22}^{(3)} J_{33}^{(3)} - J_{23}^{(3)} J_{32}^{(3)} = \frac{bem^2 z_2 y_2}{(b+y_2)^3}.$$

Thus, when

$$r_1 < d_1 + \frac{c_1 y_2}{a_1 + y_2}, \quad J_{22}^{(3)} + J_{33}^{(3)} < 0,$$

the eigenvalues of $J^{(3)}(E_{yz})$ all have negative real parts, and E_{yz} is locally asymptotically stable.

(4) If E_{yz} is in the region

$$\Delta_4 = \{(x,y,z) \in \Delta^* : \theta_1 x + z < N - qK_2, \theta_1 x + y + z > N\},$$

then $z_2 < N - qK_2$ and $y_2 + z_2 > N$. By (3.3), the Jacobian matrix of (3.1) at E_{yz} is

$$J^{(4)}(E_{yz}) = \begin{pmatrix} r_1 - d_1 - \dfrac{c_1 y_2}{a_1 + y_2} & 0 & 0 \\ -\dfrac{c_2 y_2}{a_2} & -\dfrac{r_2 y_2}{K_2} + \dfrac{m z_2 y_2}{(b+y_2)^2} & -\dfrac{m y_2}{b + y_2} \\ -\dfrac{\theta_1 emz_2}{b+y_2} & -\dfrac{em(N-z_2)z_2}{(b+y_2)^2} & -\dfrac{emz_2}{b+y_2} \end{pmatrix}.$$

The characteristic equation is

$$\left[\lambda - \left(r_1 - d_1 - \frac{c_1 y_2}{a_1 + y_2}\right)\right]\left[\lambda^2 - (J_{22}^{(4)} + J_{33}^{(4)})\lambda + J_{22}^{(4)} J_{33}^{(4)} - J_{23}^{(4)} J_{32}^{(4)}\right] = 0,$$

where $J_{ij}^{(4)}$ refers to the (i,j)-th element of $J^{(4)}(E_{yz})$ $(i,j=2,3)$, and

$$\begin{aligned}
&J_{22}^{(4)}+J_{33}^{(4)}=-\frac{r_2y_2}{K_2}+\frac{mz_2y_2}{(b+y_2)^2}-\frac{emz_2}{b+y_2},\\
&J_{22}^{(4)}J_{33}^{(4)}-J_{23}^{(4)}J_{32}^{(4)}=-\frac{emz_2}{b+y_2}\left[\frac{mz_2y_2}{(b+y_2)^2}-\frac{r_2y_2}{K_2}\right]+\frac{em^2(N-z_2)z_2y_2}{(b+y_2)^3}.
\end{aligned}$$

Thus, when

$$r_1<d_1+\frac{c_1y_2}{a_1+y_2},\quad J_{22}^{(4)}+J_{33}^{(4)}<0,\quad J_{22}^{(4)}J_{33}^{(4)}>J_{23}^{(4)}J_{32}^{(4)},$$

the eigenvalues of $J^{(4)}(E_{yz})$ all have negative real parts, and E_{yz} is locally asymptotically stable. In conclusion, if (3.23) is satisfied, then E_{yz} is locally asymptotically stable. □

The interior equilibrium of (3.1) is denoted as $E_{xyz}(x_3,y_3,z_3)$, where x_3,y_3,z_3 are solutions to the following equations:

$$\begin{cases}
r_1\left(1-\dfrac{x}{K_1}\right)-\dfrac{c_1y}{a_1+y}-d_1=0,\\
r_2\left(1-\dfrac{y}{\min\left(K_2,(N-\theta_1x-z)/q\right)}\right)-\dfrac{c_2x}{a_2+x}-\dfrac{mz}{b+y}-d_2=0,\\
e\min\left(1,\dfrac{N-\theta_1x-z}{y}\right)\dfrac{my}{b+y}-h-d_3=0.
\end{cases}\tag{3.24}$$

From (3.24), it can be seen that the interior equilibrium E_{xyz} is complex in explicit form, and its existence conditions are difficult to express explicitly. Later, numerical simulations will demonstrate the existence of E_{xyz}. The local stability of E_{xyz} is analyzed.

Theorem 3.9. *$E_{xyz}(x_3,y_3,z_3)$ is locally asymptotically stable if one of the following conditions is satisfied:*

- *(i) E_{xyz} is in region Δ_1, and $A_1<0,A_2>0$, where A_i $(i=1,2)$ are defined by* (3.26)*;*
- *(ii) E_{xyz} is in region Δ_2, and $B_1<0,B_2>0,B_3<0$, where B_i $(i=1,2)$ are defined by* (3.28)*;*
- *(iii) E_{xyz} is in region Δ_3, and $C_1<0,C_2>0,C_3>0$, where C_i $(i=1,2,3)$ are defined by* (3.30)*;*
- *(iv) E_{xyz} is in region Δ_4, and $D_1<0,D_2>0,D_3<0$, where D_i $(i=1,2)$ are defined by* (3.32).

Proof. For the stability of E_{xyz}, only the case when $K_2\le N/q$ is discussed. The case when $K_2>N/q$ can be similarly proven. The discussion is divided into the following four cases.

(1) If E_{xyz} is in the region Δ_1, where

$$\Delta_1=\{(x,y,z)\in\Delta^*:\theta_1x+z>N-qK_2,\theta_1x+y+z<N\},$$

then $\theta_1 x_3+z_3>N-qK_2, \theta_1 x_3+y_3+z_3<N$. By (3.3), the Jacobian matrix of (3.1) at E_{xyz}) is

$$J^{(1)}(E_{xyz})=\begin{pmatrix} a_{11} & a_{12} & 0\\ a_{21} & a_{22} & a_{23}\\ 0 & a_{32} & 0\end{pmatrix},$$

where

$$\begin{aligned}
&a_{11}=-\frac{r_1x_3}{K_1}, && a_{21}=-\frac{r_2\theta_1 q y_3^2}{(N-\theta_1x_3-z_3)^2}-\frac{a_2c_2y_3}{(a_2+x_3)^2},\\
&a_{12}=-\frac{a_1c_1x_3}{(a_1+y_3)^2}, && a_{22}=-\frac{qr_2y_3}{N-\theta_1x_3-z_3}+\frac{mz_3y_3}{(b+y_3)^2},\\
&a_{32}=\frac{bemz_3}{(b+y_3)^2}, && a_{23}=-\frac{r_2qy_3^2}{(N-\theta_1x_3-z_3)^2}-\frac{my_3}{b+y_3}.
\end{aligned}\tag{3.25}$$

The characteristic equation is

$$\lambda^3-(a_{11}+a_{22})\lambda^2+(a_{11}a_{22}-a_{23}a_{32}-a_{12}a_{21})\lambda+a_{11}a_{23}a_{32}=0.$$

According to the Routh-Hurwitz criterion, if

$$\begin{aligned}
&A_1\triangleq a_{11}+a_{22}<0,\\
&A_2\triangleq (a_{11}+a_{22})(a_{12}a_{21}-a_{11}a_{22})+a_{22}a_{23}a_{32}>0,
\end{aligned}\tag{3.26}$$

then all eigenvalues of $J^{(1)}(E_{xyz})$ have negative real parts, and E_{xyz} is locally asymptotically stable.

(2) If E_{xyz} is in the region Δ_2, where

$$\Delta_2=\{(x,y,z)\in\Delta^*:\theta_1x+z>N-qK_2,\theta_1x+y+z>N\},$$

then $\theta_1x_3+z_3>N-qK_2, \theta_1x_3+y_3+z_3>N$. By (3.3), the Jacobian matrix of (3.1) at E_{xyz} is

$$J^{(2)}(E_{xyz})=\begin{pmatrix} b_{11} & b_{12} & 0\\ b_{21} & b_{22} & b_{23}\\ b_{31} & b_{32} & b_{33}\end{pmatrix},$$

where

$$\begin{aligned}
&b_{11}=-\frac{r_1x_3}{K_1}, && b_{12}=-\frac{a_1c_1x_3}{(a_1+y_3)^2},\\
&b_{21}=-\frac{r_2\theta_1qy_3^2}{(N-\theta_1x_3-z_3)^2}-\frac{a_2c_2y_3}{(a_2+x_3)^2}, && b_{22}=-\frac{qr_2y_3}{N-\theta_1x_3-z_3}+\frac{mz_3y_3}{(b+y_3)^2},\\
&b_{23}=-\frac{r_2qy_3^2}{(N-\theta_1x_3-z_3)^2}-\frac{my_3}{b+y_3}, && b_{31}=-\frac{\theta_1emz_3}{b+y_3},\\
&b_{32}=-\frac{em(N-\theta_1x_3-z_3)z_3}{(b+y_3)^2}, && b_{33}=-\frac{emz_3}{b+y_3}.
\end{aligned}\tag{3.27}$$

The characteristic equation is

$$\begin{aligned}&\lambda^3-(b_{11}+b_{22}+b_{33})\lambda^2+(b_{11}b_{22}+b_{11}b_{33}+b_{22}b_{33}-b_{23}b_{32}-b_{12}b_{21})\lambda\\&\quad+(b_{11}b_{22}b_{33}+b_{23}b_{32}b_{11}+b_{12}b_{21}b_{33}-b_{12}b_{23}b_{31})=0.\end{aligned}$$

According to the Routh-Hurwitz criterion, if

$$\begin{aligned}&B_1\triangleq b_{11}+b_{22}+b_{33}<0,\\&B_2\triangleq b_{11}b_{22}b_{33}+b_{23}b_{32}b_{11}+b_{12}b_{21}b_{33}-b_{12}b_{23}b_{31}>0,\\&B_3\triangleq (b_{11}+b_{22}+b_{33})(b_{11}b_{22}+b_{11}b_{33}+b_{22}b_{33}-b_{23}b_{32}-b_{12}b_{21})\\&\qquad+b_{11}b_{22}b_{33}+b_{23}b_{32}b_{11}+b_{12}b_{21}b_{33}-b_{12}b_{23}b_{31}<0,\end{aligned}\tag{3.28}$$

then all eigenvalues of $J^{(2)}(E_{xyz})$ have negative real parts, and E_{xyz} is locally asymptotically stable.

(3) If E_{xyz} is in the region Δ_3, where

$$\Delta_3=\{(x,y,z)\in\Delta^*:\theta_1x+z<N-qK_2,\theta_1x+y+z<N\},$$

then $\theta_1x_3+z_3<N-qK_2,\theta_1x_3+y_3+z_3<N$. By (3.3), the Jacobian matrix of (3.1) at E_{xyz} is

$$J^{(3)}(E_{xyz})=\begin{pmatrix}c_{11}&c_{12}&0\\c_{21}&c_{22}&c_{23}\\0&c_{32}&0\end{pmatrix},$$

where

$$\begin{aligned}&c_{11}=-\frac{r_1x_3}{K_1}, &&c_{12}=-\frac{a_1c_1x_3}{(a_1+y_3)^2}, &&c_{21}=-\frac{a_2c_2y_3}{(a_2+x_3)^2},\\&c_{22}=-\frac{r_2y_3}{K_2}+\frac{mz_3y_3}{(b+y_3)^2}, &&c_{23}=-\frac{my_3}{b+y_3}, &&c_{32}=\frac{bemz_3}{(b+y_3)^2}.\end{aligned}\tag{3.29}$$

The characteristic equation is

$$\lambda^3-(c_{11}+c_{22})\lambda^2+(c_{11}c_{22}-c_{23}c_{32}-c_{12}c_{21})\lambda+c_{11}c_{23}c_{32}=0.$$

According to the Routh-Hurwitz criterion, if

$$\begin{aligned}&C_1\triangleq c_{11}+c_{22}<0,\\&C_2\triangleq (c_{11}+c_{22})(c_{12}c_{21}-c_{11}c_{22})+c_{22}c_{23}c_{32}>0,\end{aligned}\tag{3.30}$$

then all eigenvalues of $J^{(3)}(E_{xyz})$ have negative real parts, and E_{xyz} is locally asymptotically stable.

(4) If E_{xyz} is in the region Δ_4, where

$$\Delta_4=\{(x,y,z)\in\Delta^*:\theta_1x+z<N-qK_2,\theta_1x+y+z>N\},$$

then $\theta_1x_3+z_3<N-qK_2,\theta_1x_3+y_3+z_3>N$. By (3.3), the Jacobian matrix of (3.1) at E_{xyz} is

$$J^{(4)}(E_{xyz})=\begin{pmatrix} d_{11} & d_{12} & 0\\ d_{21} & d_{22} & d_{23}\\ d_{31} & d_{32} & d_{33}\end{pmatrix},$$

where

$$\begin{aligned} &d_{11}=-\frac{r_1x_3}{K_1}, && d_{12}=-\frac{a_1c_1x_3}{(a_1+y_3)^2}, && d_{21}=-\frac{a_2c_2y_3}{(a_2+x_3)^2},\\ &d_{22}=-\frac{r_2y_3}{K_2}+\frac{mz_3y_3}{(b+y_3)^2}, && d_{23}=-\frac{my_3}{b+y_3}, && d_{31}=-\frac{\theta_1emz_3}{b+y_3},\\ &d_{32}=-\frac{em(N-\theta_1x_3-z_3)z_3}{(b+y_3)^2}, && d_{33}=-\frac{emz_3}{b+y_3}. \end{aligned} \tag{3.31}$$

The characteristic equation is

$$\begin{aligned} &\lambda^3-(d_{11}+d_{22}+d_{33})\lambda^2+(d_{11}d_{22}+d_{11}d_{33}+d_{22}d_{33}-d_{23}d_{32}-d_{12}d_{21})\lambda\\ &\quad+(d_{11}d_{22}d_{33}+d_{23}d_{32}d_{11}+d_{12}d_{21}d_{33}-d_{12}d_{23}d_{31})=0. \end{aligned}$$

According to the Routh-Hurwitz criterion, if

$$\begin{aligned} &D_1\triangleq d_{11}+d_{22}+d_{33}<0,\\ &D_2\triangleq d_{11}d_{22}d_{33}+d_{23}d_{32}d_{11}+d_{12}d_{21}d_{33}-d_{12}d_{23}d_{31}>0,\\ &D_3\triangleq(d_{11}+d_{22}+d_{33})(d_{11}d_{22}+d_{11}d_{33}+d_{22}d_{33}-d_{23}d_{32}-d_{12}d_{21})\\ &\qquad+d_{11}d_{22}d_{33}+d_{23}d_{32}d_{11}+d_{12}d_{21}d_{33}-d_{12}d_{23}d_{31}<0, \end{aligned} \tag{3.32}$$

then all eigenvalues of $J^{(4)}(E_{xyz})$ have negative real parts, and E_{xyz} is locally asymptotically stable. □

The criteria for the existence and stability of equilibria of (3.1) are summarized in Table 2.

4 Numerical simulations

In this section, numerical simulations are employed to illustrate the stability conditions of the equilibria of (2.5), showcasing the complex dynamical behaviors among corals, macroalgae, and herbivorous fish. The effects of light, nutrients, and harvesting on population dynamics are also well explored.

Table 2: Equilibrium analysis of (3.1).

E	Criteria for Existence	Criteria for Stability	Stability
E_0	Always exists	$r_1<d_1, r_2<d_2$	GAS
E_x	$r_1>d_1$	$r_2<d_2+\dfrac{c_2K_1(r_1-d_1)}{r_1a_2+(r_1-d_1)K_1}$ $r_2<d_2$	LAS GAS
E_y	$r_2>d_2$	$r_1<d_1+\dfrac{c_1k(r_2-d_2)}{r_2a_1+(r_2-d_2)k}$, $h+d_3>\max\left\{\dfrac{em(r_2-d_2)k}{r_2b+(r_2-d_2)k},\dfrac{emr_2N}{r_2b+(r_2-d_2)k}\right\}$ $r_1<d_1$, $h+d_3>\max\left\{\dfrac{em(r_2-d_2)k}{r_2b+(r_2-d_2)k},\dfrac{emr_2N}{r_2b+(r_2-d_2)k}\right\}$	LAS GAS
E_{xy}	$r_1>d_1, r_2>d_2$, $K_1>\max\{S_1,S_3\}, k>S_2$	$h+d_3>\max\left\{\frac{emy_1}{b+y_1},\frac{em(N-\theta_1x_1)}{b+y_1}\right\}$ $J_{11}^{(k)}J_{22}^{(k)}>J_{12}^{(k)}J_{21}^{(k)}$ $(k=1,3)$ $h+d_3>me$, $r_2>d_2+\dfrac{c_2K_1(r_1-d_1)}{r_1a_2+(r_1-d_1)K_1}$, $r_1>d_1+\dfrac{c_1k(r_2-d_2)}{r_2a_1+(r_2-d_2)k}$	LAS GAS
E_{yz}	—	$r_1<d_1+\dfrac{c_1y_2}{a_1+y_2}$, $J_{22}^{(k)}+J_{33}^{(k)}<0$ $(k=1,\dots,4)$, $J_{22}^{(l)}J_{33}^{(l)}>J_{23}^{(l)}J_{32}^{(l)}$ $(l=1,2)$	LAS
E_{xyz}	—	$A_1<0, A_2>0;$ $B_1<0, B_2>0, B_3<0;$ $C_1<0, C_2>0;$ $D_1<0, D_2>0, D_3<0$	LAS

Here LAS and GAS denote locally and globally asymptotic stability, respectively.

4.1 Rich dynamics

From the above analyses, it is observed that (2.5) admits very rich dynamics. For example,

- when the intrinsic growth rates of corals and macroalgae are both low, all three species (corals, macroalgae, and herbivorous fish) go extinct (see Fig. 2(a));

- when the intrinsic growth rate of corals is high and that of macroalgae is low, only corals survive, while macroalgae and herbivorous fish go extinct (see Fig. 2(b));
- when the intrinsic growth rate of corals is low, the intrinsic growth rate of macroalgae is high, and the sum of the mortality and harvesting rates of herbivorous fish is also high, only macroalgae survive, while corals and herbivorous fish go extinct (see Fig. 2(c));
- corals and macroalgae coexist, while herbivorous fish go extinct (see Fig. 2(d));
- macroalgae and herbivorous fish coexist, while corals go extinct (see Fig. 2(e));
- corals, macroalgae, and herbivorous fish coexist (see Fig. 2(f)).

Moreover, the impact of initial conditions on the interior equilibrium point of system (2.5) is investigated (see Fig. 3). It can be observed that the solution trajectories of the system with different initial conditions all converge to the interior equilibrium, illustrating the stability of the system near the interior equilibrium. The specific parameter values are provided in Table 3 for Fig. 2(f).

System (2.5) exhibits bistable behavior (as shown in Fig. 4). Under the same parameter settings but with different initial conditions, the system may stabilize in either a state where only corals persist while macroalgae and herbivorous fish go extinct, or a state where corals go extinct while macroalgae and herbivorous fish coexist. Furthermore, transitions between these two states are possible. This indicates that the dynamical behavior of system (2.5) is sensitive to initial conditions.

In addition, by varying the parameter values of system (2.5), it is observed that the system also exhibits different types of periodic oscillatory behavior (as shown in Fig. 5):

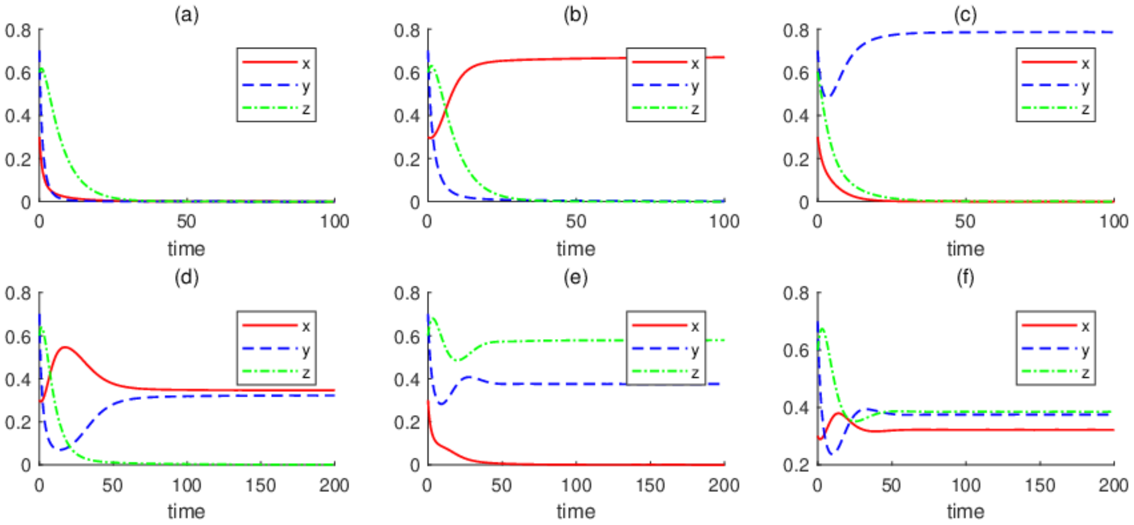

Figure 2: Attractor of (2.5). (a) E_0, (b) E_x, (c) E_y, (d) E_{xy}, (e) E_{yz},(f) E_{xyz}. The parameter values are listed in Table 3, and the initial value is set to be $(0.3,0.7,0.6)$.

Table 3: Parameter values of (2.5) in Fig. 2.

	Parameter values	Dynamical behavior
Fig. 2(a)	$r_1=0.5, K_1=0.7, r_2=0.6, K_2=0.8, c_1=0.75$, $a_1=0.3$, $d_1=0.6$, $c_2=0.3$, $a_2=0.3$, $d_2=0.7$, $m=1$, $b=1.5$, $e=0.8$, $d_3=0.01$, $h=0.15$, $N=0.35$, $\theta_1=0.2$, $\theta_2=0.2$, $q=0.064$.	E_0 is an attractor, i.e. corals, macroalgae, and herbivorous fish all go extinct.
Fig. 2(b)	$r_1=0.5$, $K_1=0.7$, $r_2=0.6$, $K_2=0.8$, $c_1=0.45$, $a_1=0.3$, $d_1=0.02$, $c_2=0.89$, $a_2=0.3$, $d_2=0.01$, $m=1$, $b=1.5$, $e=0.8$, $d_3=0.01$, $h=0.15$, $N=0.35$, $\theta_1=0.2$, $\theta_2=0.2$, $q=0.064$.	E_x is an attractor, i.e. corals persist stably, while macroalgae and herbivorous fish go extinct.
Fig. 2(c)	$r_1=0.5$, $K_1=0.7$, $r_2=0.6$, $K_2=0.8$, $c_1=0.95$, $a_1=0.3$, $d_1=0.02$, $c_2=0.2$, $a_2=0.3$, $d_2=0.01$, $m=1$, $b=1.5$, $e=0.8$, $d_3=0.01$, $h=0.38$, $N=0.35$, $\theta_1=0.2$, $\theta_2=0.2$, $q=0.064$.	E_y is an attractor, i.e. macroalgae persist stably, while corals and herbivorous fish go extinct.
Fig. 2(d)	$r_1=0.5$, $K_1=0.7$, $r_2=0.6$, $K_2=0.8$, $c_1=0.45$, $a_1=0.3$, $d_1=0.02$, $c_2=0.65$, $a_2=0.3$, $d_2=0.01$, $m=1$, $b=1.5$, $e=0.8$, $d_3=0.01$, $h=0.15$, $N=0.35$, $\theta_1=0.2$, $\theta_2=0.2$, $q=0.064$.	E_{xy} is an attractor, i.e. herbivorous fish go extinct, while corals and macroalgae stably coexist.
Fig. 2(e)	$r_1=0.5$, $K_1=0.7$, $r_2=0.6$, $K_2=0.8$, $c_1=0.95$, $a_1=0.3$, $d_1=0.02$, $c_2=0.2$, $a_2=0.3$, $d_2=0.01$, $m=1$, $b=1.5$, $e=0.8$, $d_3=0.01$, $h=0.15$, $N=0.35$, $\theta_1=0.2$, $\theta_2=0.2$, $q=0.064$.	E_{yz} is an attractor, i.e. corals go extinct, while macroalgae and herbivorous fish stably coexist.
Fig. 2(f)	$r_1=0.5$, $K_1=0.7$, $r_2=0.6$, $K_2=0.8$, $c_1=0.45$, $a_1=0.3$, $d_1=0.02$, $c_2=0.2$, $a_2=0.3$, $d_2=0.01$, $m=1$, $b=1.5$, $e=0.8$, $d_3=0.01$, $h=0.15$, $N=0.35$, $\theta_1=0.2$, $\theta_2=0.2$, $q=0.064$.	E_{xyz} is an attractor, i.e. corals, macroalgae, and herbivorous fish stably coexist.

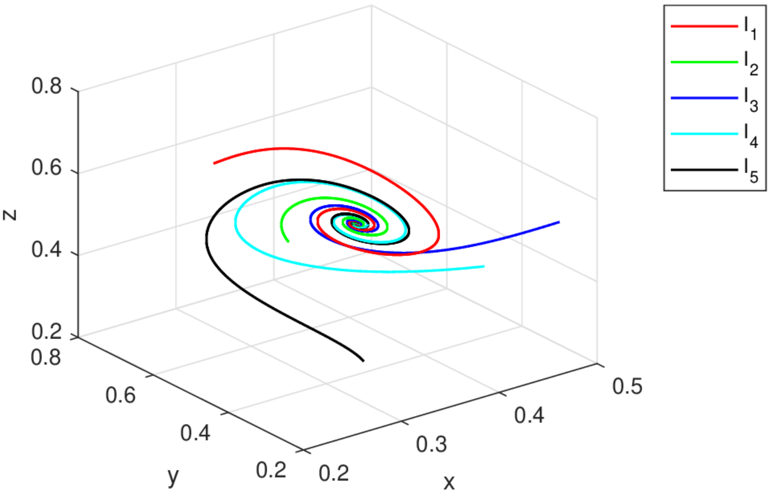

Figure 3: System (2.5) with an asymptotically stable interior equilibrium. The corresponding initial conditions are $I_1=(0.3,0.7,0.6)$, $I_2=(0.3,0.5,0.5)$, $I_3=(0.5,0.3,0.5)$, $I_4=(0.5,0.5,0.3)$, $I_5=(0.3,0.3,0.3)$.

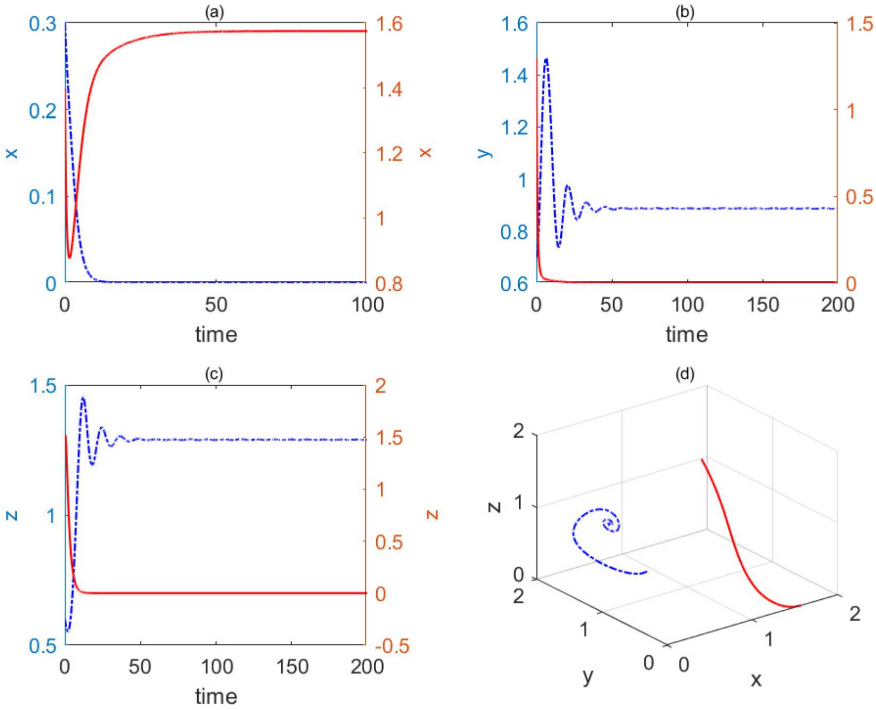

Figure 4: Bistable scenario of system (2.5). The solid red line corresponds to the initial condition $(0.3,0.7,0.6)$, where corals persist, and macroalgae and herbivorous fish go extinct. The dashed blue line corresponds to the initial condition $(1.4,1.3,1.5)$, where corals go extinct, and macroalgae and herbivorous fish coexist. The parameter values are $r_1=0.6, K_1=2.1, r_2=1.7, K_2=2.5, c_1=1.8, a_1=1.3, d_1=0.15, c_2=3, a_2=1.3, d_2=0.17, m=1.5, b=1.2, e=0.8, d_3=0.26, h=0.25, N=3.5, \theta_1=0.2, \theta_2=0.2, q=0.064$.

periodic oscillations where macroalgae and herbivorous fish coexist while corals go extinct, and periodic oscillations where corals, macroalgae, and herbivorous fish coexist.

4.2 Effect of light on dynamics

In coral reefs, the canopy formed by the aggregation of macroalgae shades the underlying area, reducing light intensity beneath the canopy. The parameter K_2 represents the carrying capacity of macroalgae limited by light. Therefore, the light intensity in coral reefs can be characterized by K_2. Moreover, light and nutrients are critical factors affecting the dynamics of aquatic ecosystems. This subsection uses numerical analysis to explore the effects of light intensity and nutrients on population dynamics in coral reefs. Unless otherwise specified, the parameter values in this subsection are taken from Table 3 for Fig. 2(f), with the initial condition $(0.3,0.7,0.6)$.

Fig. 6 illustrates the effect of light intensity K_2 on the dynamics of (2.5). When the light intensity is low $(0<K_2<0.47)$, corals and macroalgae survive in the system, while herbivorous fish go extinct. In this scenario, the low light intensity implies that the energy fixed by macroalgae through photosynthesis is insufficient to support the survival of

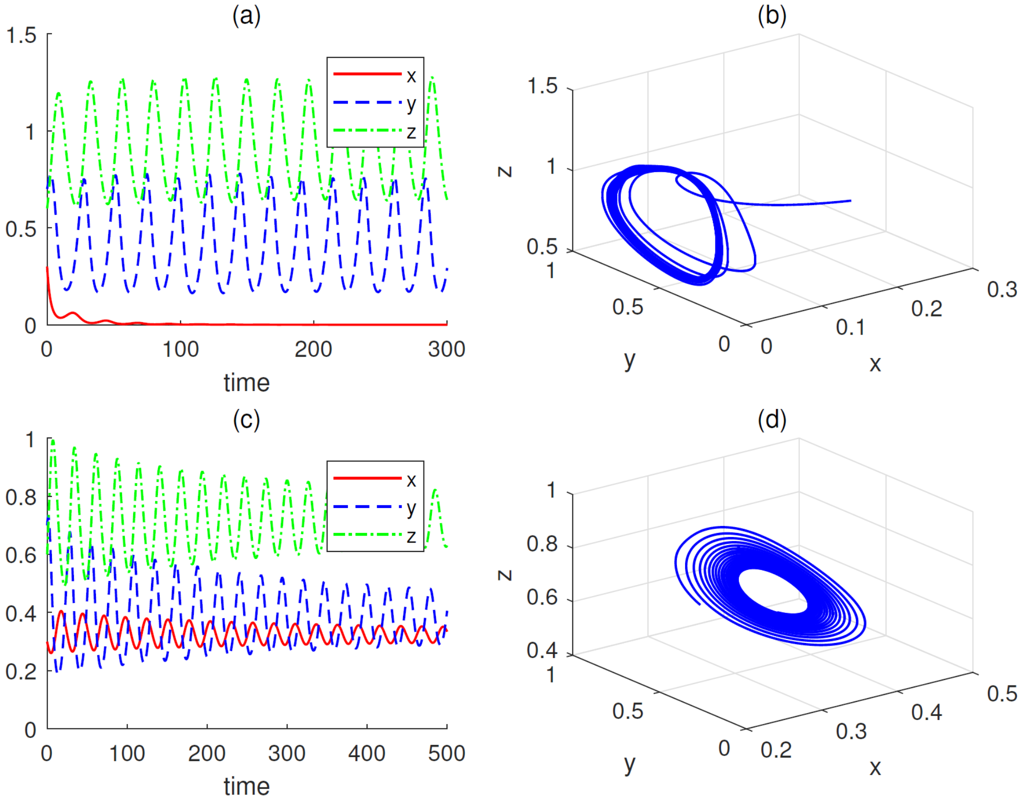

Figure 5: Oscillatory dynamical behavior of system (2.5). (a-b) Macroalgae and herbivorous fish coexist in periodic oscillations, while corals go extinct, here $r_1=0.5$, $K_1=0.7, r_2=0.6, K_2=3.5, c_1=0.95, a_1=0.3$, $d_1=0.02, c_2=0.2, a_2=0.3, d_2=0.01, m=1, b=1.5, e=0.8, d_3=0.01, h=0.15, N=0.35, \theta_1=0.2, \theta_2=0.2, q=0.064$. (c-d) Corals, macroalgae, and herbivorous fish coexist in periodic oscillations, here $r_1=0.5, K_1=0.7, r_2=0.6$, $K_2=3.5, c_1=0.45, a_1=0.3, d_1=0.02, c_2=0.2, a_2=0.3, d_2=0.01, m=1, b=1.5, e=0.8, d_3=0.01, h=0.15, N=0.35$, $\theta_1=0.2, \theta_2=0.2, q=0.064$. The initial conditions are all set to be $(0.3,0.7,0.6)$.

herbivorous fish. Meanwhile, the biomass of macroalgae at equilibrium increases with light intensity. This growth and aggregation of macroalgae exert competitive inhibitory effects on coral growth, causing the biomass of corals at equilibrium to decrease as light intensity increases.

When light intensity increases further ($0.47<K_2<1.9$), the three populations coexist. In this case, the energy fixed by macroalgae through photosynthesis becomes sufficient to support the survival of herbivorous fish. As a result, the biomass of herbivorous fish at equilibrium increases with light intensity. When light intensity continues to increase ($K_2>1.9$), the coexistence of the three populations becomes unstable, manifesting as oscillatory coexistence.

Fig. 7 shows the solution trajectories under different values of K_2, providing further insight into the impact of light intensity on system (2.5). When light intensity is low, by comparing Figs. 7(a) ($K_2=0.1$) and 7(b) ($K_2=0.3$), it is evident that as K_2 increases, the

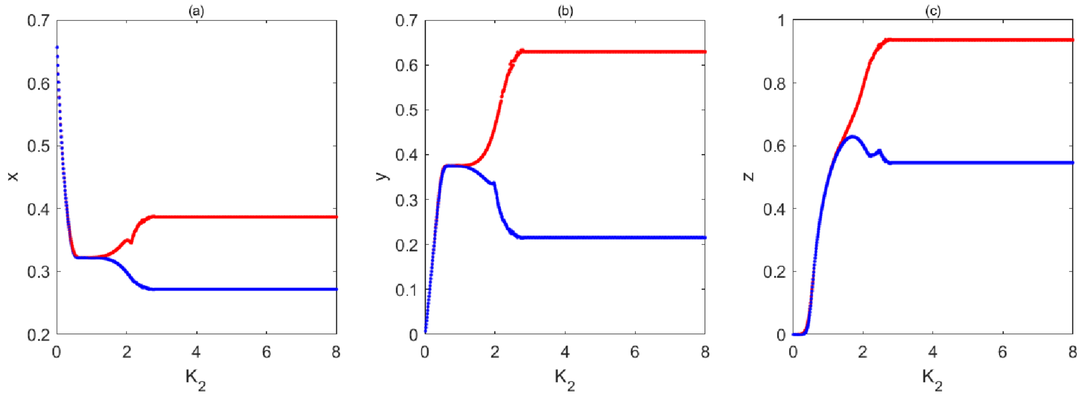

Figure 6: Bifurcation diagram of system (2.5) with respect to K_2, where $N=0.35$.

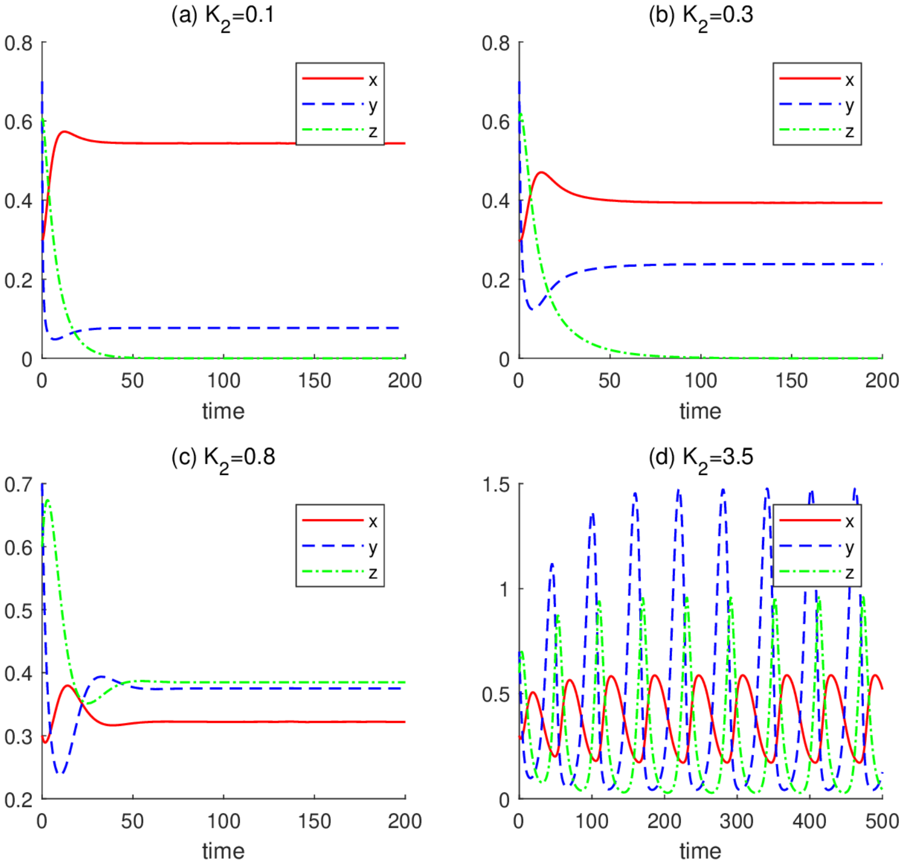

Figure 7: Effect of light intensity K_2 on system (2.5). Except for the parameters under discussion, other parameter values are taken from Table 3 for Fig. 2(f).

biomass of macroalgae increases while the biomass of corals decreases. Fig. 7(c) illustrates the case with $K_2=0.8$, showing that all three populations coexist stably, with the biomass of macroalgae exceeding that of corals. Fig. 7(d) depicts the case with $K_2=3.5$, where the system loses stability, and the three populations cyclicly coexist. The amplitude of oscillations for macroalgae is greater than that of corals.

In summary, as the light intensity increases, macroalgae gains a competitive advantage over corals, gradually dominating the coral reef. Moreover, under high light intensity, the survival of macroalgae is less stable compared to corals.

4.3 Combined effects of light and nutrients

Nutrient is critical limiting factor for biological growth. The effect of nutrient concentration N on population dynamics in system (2.5) is investigated. Fig. 8 shows that, when $N=0.2$ and $K_2>1.9$, the three populations coexist in a stable state. Fig. 9 illustrates that, when $N=0.29$ and $K_2>1.9$, the three populations coexist in an oscillatory state with smaller amplitudes. Meanwhile, Fig. 6 shows that, when $N=0.35$ and $K_2>1.9$, the three populations coexist in an oscillatory state with larger amplitudes.

In other words, N amplifies the impact of K_2 on population dynamics. As N increases, the amplitude of cyclic oscillation in the bifurcation diagram with respect to light intensity K_2 becomes larger, and the instability of the system becomes more pronounced. In summary, an increase in nutrients affects the effect of light intensity on the system, making it less favorable for the system's stability.

By comparing Figs. 10(a) and 10(b), one can also observe that, when N is smaller, the time required for the biomass of three populations to reach stability is shorter; when N is larger, the time required for the biomass of three populations to reach stability is longer. This indicates that the system stabilizes faster when nutrient content is lower.

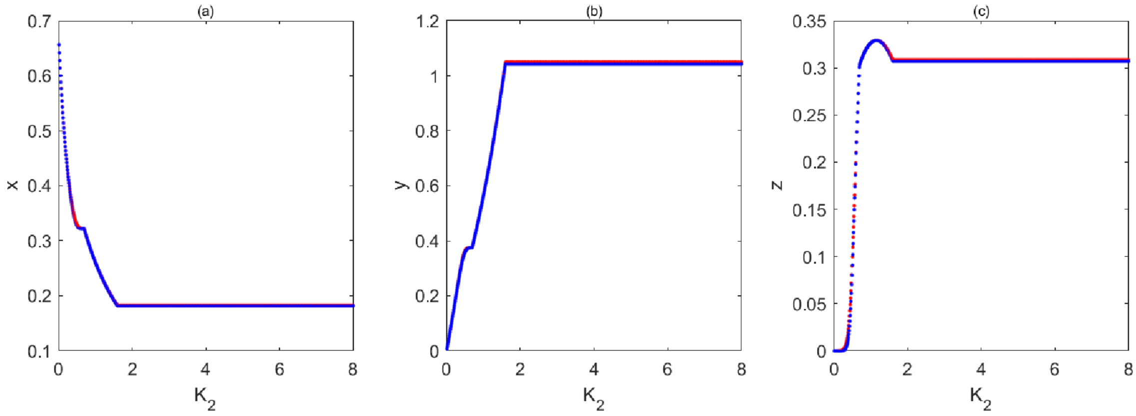

Figure 8: Bifurcation diagram of system (2.5) with respect to K_2, where $N=0.2$.

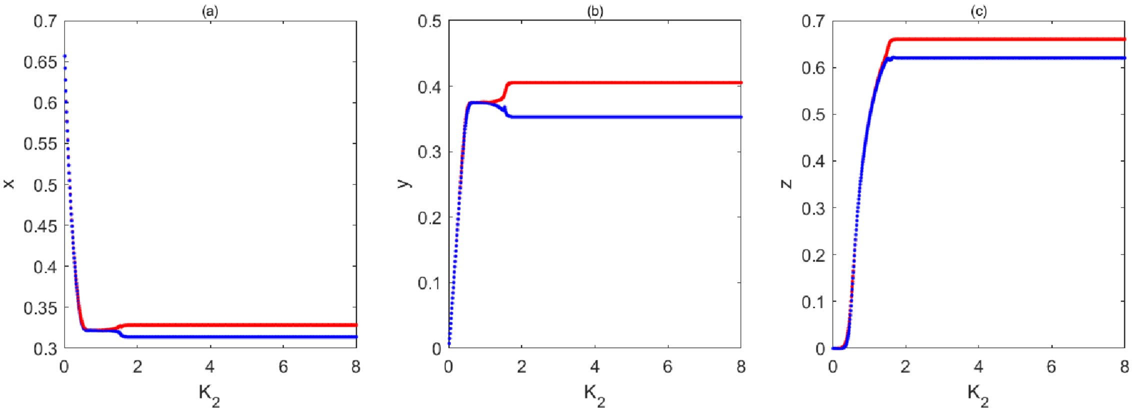

Figure 9: Bifurcation diagram of system (2.5) with respect to K_2, where $N=0.29$.

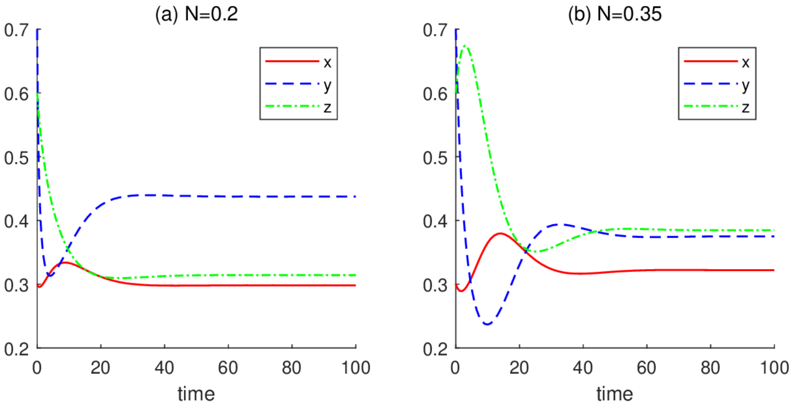

Figure 10: Effect of nutrient content N on system (2.5). Except for the parameters under discussion, other parameter values are taken from Table 3(f).

4.4 Effect of harvesting on dynamics

Overfishing of herbivorous fish is a primary driver of phase shifts in coral reefs. This subsection explores the impact of the harvesting rate of herbivorous fish on the dynamical behavior of system (2.5) through numerical simulations. Unless otherwise specified, the parameter values in this subsection are taken from Table 3 for Fig. 2(f) with the initial condition $(0.3,0.7,0.6)$.

Overfishing of herbivorous fish can lead to a phase shift from coral dominance to macroalgae dominance. The bifurcation diagram Fig. 11 illustrates the effect of the harvesting rate h on the dynamics of (2.5). When the harvesting intensity is low $(0<h<0.17)$, three populations coexist in oscillatory dynamics. As the harvesting intensity increases further $(0.17<h<0.41)$, three populations coexist stably. During this phase, as the harvesting intensity increases, grazing pressure from herbivorous fish on macroalgae decreases, allowing macroalgae to proliferate and suppress coral's recruitment. Consequently, the

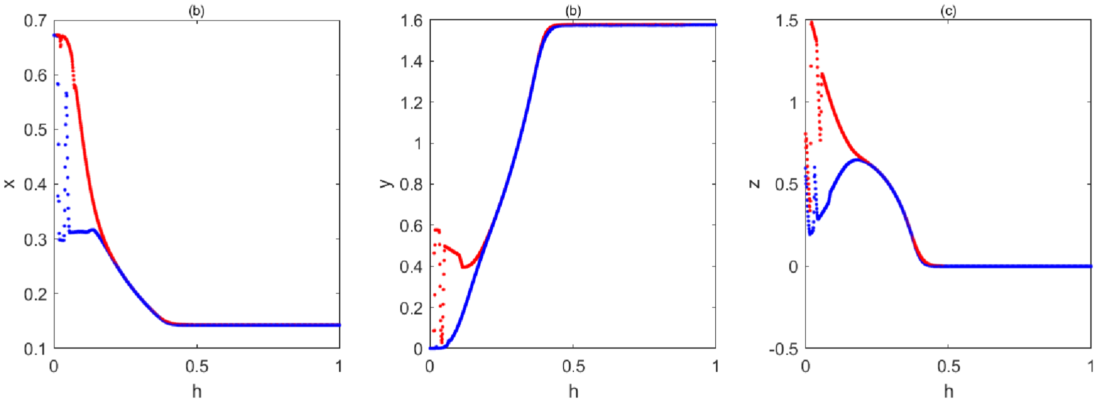

Figure 11: Bifurcation diagram of system (2.5) with respect to h.

biomass of corals and herbivorous fish decreases, while the biomass of macroalgae increases. When the harvesting intensity continues to rise ($h > 0.41$), corals and macroalgae survive in the system, while herbivorous fish go extinct, and macroalgae dominate the system.

Fig. 12 shows the solution trajectories of (2.5) for different values of h, providing further insight into the effect of the harvesting intensity of herbivorous fish on system (2.5). Fig. 12 demonstrates that, when $h = 0.03$, three populations coexist in oscillatory dynamics; when $h = 0.2$ and $h = 0.3$, three populations coexist stably; when $h = 0.45$, corals and macroalgae coexist while herbivorous fish go extinct. It is revealed that, under higher harvesting intensities, the population dynamics shift from oscillatory to stable, and excessive harvesting can lead to the extinction of herbivorous fish.

By comparing Figs. 12(b), 12(c), and 12(d), it is evident that, as harvesting intensity increases, the biomass of macroalgae increases significantly, while the biomass of corals decreases. This fact indicates that the loss of herbivorous fish due to harvesting facilitates the growth of macroalgae, which in turn reduces coral coverage. In other words, overfishing is detrimental to coral-dominated reefs. This finding aligns with the results of most field and empirical studies.

To sum up, in this section, it first observes through numerical simulations that system (2.5) exhibits rich dynamical behaviors such as bistability and different types of periodic oscillations. Second, the effect of light intensity on the dynamics of (2.5) is deliberately explored and it is shown that, increased light intensity leads to macroalgae dominating the coral reef and, beyond a certain threshold, causes periodic oscillations that destabilize the populations. In addition, the combined effects of light intensity and nutrients are discussed, revealing that increased nutrient levels amplify the effect of light intensity, making the coexistence equilibrium of three populations less stable. Finally, the effect of the harvesting intensity of herbivorous fish on the system is explored, indicating that, as harvesting intensity increases, coral reefs transition from being coral-dominated to macroalgae-dominated.

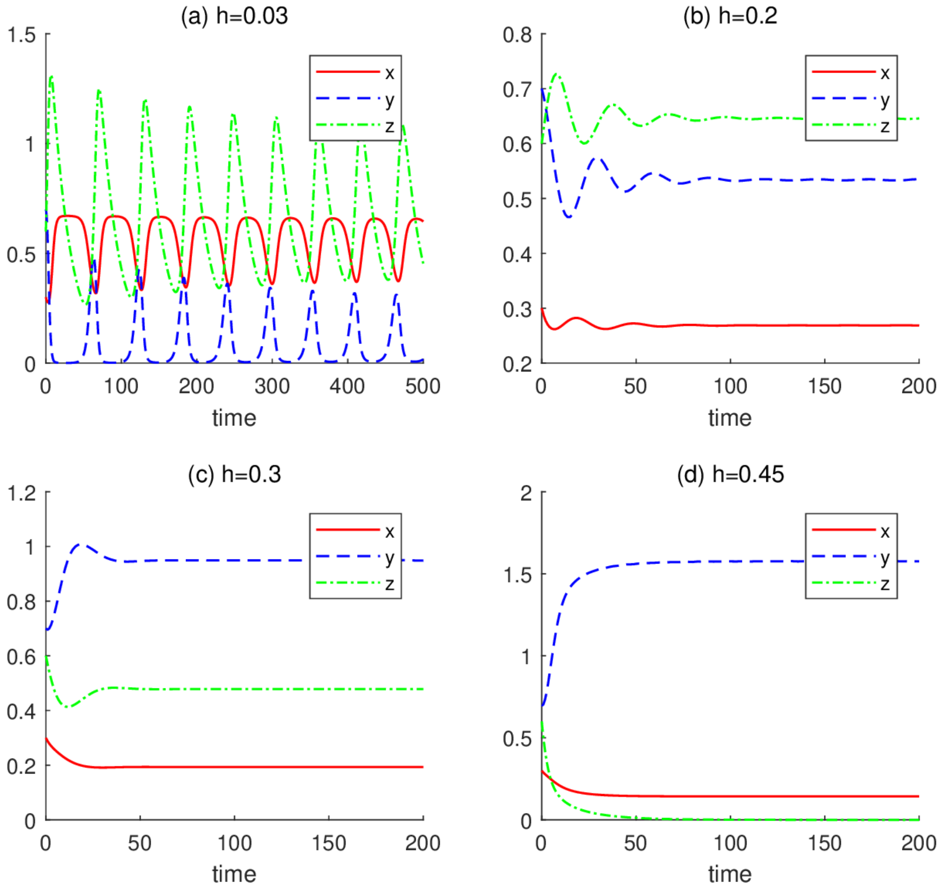

Figure 12: Effect of harvesting intensity h on system (2.5). Except for the parameters under discussion, other parameter values are taken from Table 3.

The obtained results provide several advantages in understanding coral-algae dynamics. First, by incorporating nutrient constraints through ecological stoichiometry, the model captures the joint effects of energy and nutrient limitations on macroalgae and herbivorous fish, offering a more realistic and mechanistic description of trophic interactions. Then the analytical results give clear conditions for the existence and global stability of different equilibria, enabling precise ecological interpretations such as thresholds for coral extinction or macroalgal dominance. Moreover, the model reveals complex dynamical behaviors like bistability and oscillations, which are crucial for identifying early warning signals of regime shifts.

However, the model also has some limitations. It assumes a closed nutrient system without external nitrogen inputs or losses, which may not fully capture the open nature of coastal ecosystems. In addition, spatial heterogeneity and diffusion processes are not considered, and the model treats fish grazing as homogeneous across the reef. These simplifications, while mathematically tractable, may limit the direct applicability of the results to highly heterogeneous or strongly disturbed reef systems. Future work may address these issues by incorporating spatial dynamics, temporal variability in nutrient input, or more complex feeding behavior.

5 Conclusion

In recent years, coral-algal phase shift driven by environmental stressors including light intensity variations, eutrophication, and overfishing has been recognized as critical threats to coral reef resilience. While most existing studies focus on herbivorous reef fish regulation, the substantial effects of nutrient stoichiometric variability on population dynamics remain understudied. To resolve this knowledge gap, the theory of ecological stoichiometry is employed to develop a dynamical model incorporating corals, macroalgae, and herbivorous fish. The underlying mechanisms by which environmental factors drive the phase shifts in coral reef ecosystems are well explored.

Theoretical analyses and numerical simulations elucidate how crucial parameters affect coral reef ecosystems. When coral and macroalgae intrinsic growth rates fall below mortality rates, both populations converge to extinction (E_0), reflecting reef collapse under environmental stress. A higher intrinsic growth rate compared to mortality rates predisposes corals towards achieving dominance (E_x). The macroalgae-dominated state (E_y) and multi-species coexistence states (E_{xy}, E_{yz}, E_{xyz}) are constrained by multiple factors, including their growth and mortality rates, nutrient limitations, and herbivory pressure. Increasing light intensity induces phase shift from coral-dominated to macroalgal-dominated states, with superthreshold intensities generating sustained oscillations. Eutrophication synergistically amplifies light effects, reducing system resilience. Overfishing diminishes herbivorous fish grazing pressure, constituting a key phase shift driver. Collectively, the combined effects of human activities and natural disturbances drive phase shifts, compromising ecosystem structure and ecological function. These results establish bifurcation thresholds for state transitions, informing restoration strategies including fisheries management and nutrient input regulation.

Fear effect as a key regulatory factor in consumer foraging ecology. Population size mediates this effect through density-dependent feedback mechanisms. In coral reef ecosystems, fear effect alters browser fish grazing rates that maintain keystone control over fleshy macroalgal proliferation. Developing ecological stoichiometry models incorporating fear effects will elucidate mechanisms driving coral-macroalgae phase shifts and establish quantitative frameworks for conservation strategies. Furthermore, the current model focuses on carbon and nitrogen under a closed nitrogen cycle, excluding the stoichiometric constraints from phosphorus, sulfur, and calcium, as well as free nitrogen in the environment. Future studies should extend to non-closed nitrogen systems and comprehensively combined effects of multiple chemical elements.

As a critical component of marine biodiversity, the health of coral reef ecosystems is intricately linked to global ecological balance and human well-being. The 2025 “A Survey

Report on the Coral Reef Ecosystems of Tiexian Jiao and Niu'e Jiao" evaluated the status of these coral reef ecosystems [43]. The findings indicate a decline in the coverage of reef-building corals, with the Tiexian Jiao exhibiting particularly severe degradation. With the continued rise in sea surface temperatures, coral reef ecosystems are facing the potential risk of mass coral bleaching. To prevent further degradation of coral reefs, it is imperative to deepen the studies on the driving mechanisms of environmental factors on coral reef ecosystems and to implement human interventions to mitigate the negative effects of external factors on coral reefs, thereby promoting the recovery and development of coral reef ecosystems.

Acknowledgements

This research is supported by the National Natural Science Foundation of P.R. China (Grant Nos. 12471456 and 12401636), by the Natural Science Foundation (Grant No. ZR2024QA038) and by the Taishan Scholars Program of Shandong Province of P.R. China, and by the University-level General Projects of Bohai University (Grant No. 0525xn087).

References

[1] K. R. N. Anthony, J. A. Maynard, G. Diaz-Pulido, P. J. Mumby, P. A. Marshall, L. Cao, and O. Hoegh-Guldberg, *Ocean acidification and warming will lower coral reef resilience*, Glob. Change Biol., 17(5):1798–1808, 2011.

[2] J. E. Arias-González, T. Fung, R. M. Seymour, J. R. Garza-Pérez, G. Acosta-González, Y.-M. Bozec, and C. R. Johnson, *A coral-algal phase shift in Mesoamerica not driven by changes in herbivorous fish abundance*, PLoS One, 12(4):e0174855, 2017.

[3] J. J. Bell, *The functional roles of marine sponges*, Estuar. Coast. Shelf Sci., 79(3):341–353, 2008.

[4] J. Bhattacharyya and S. Pal, *Hysteresis in coral reefs under macroalgal toxicity and overfishing*, J. Biol. Phys., 41(2):151–172, 2015.

[5] J. C. Blackwood, A. Hastings, and P. J. Mumby, *A model-based approach to determine the longterm effects of multiple interacting stressors on coral reefs*, Ecol. Appl., 21(7):2722–2733, 2011.

[6] J. C. Blackwood, A. Hastings, and P. J. Mumby, *The effect of fishing on hysteresis in Caribbean coral reefs*, Theor. Ecol., 5(1):105–114, 2012.

[7] R. Bouterfas, M. Belkoura, and A. Dauta, *Light and temperature effects on the growth rate of three freshwater algae isolated from a eutrophic lake*, Hydrobiologia, 489(1):207–217, 2002.

[8] R. M. Brooker, S. J. Brandl, and D. L. Dixson, *Cryptic effects of habitat declines: Coral-associated fishes avoid coral-seaweed interactions due to visual and chemical cues*, Sci. Rep., 6(1):18842, 2016.

[9] J. F. Bruno, H. Sweatman, W. F. Precht, E. R. Selig, and V. G. W. Schutte, *Assessing evidence of phase shifts from coral to macroalgal dominance on coral reefs*, Ecology, 90(6):1478–1484, 2009.

[10] A. J. Cheal, M. A. MacNeil, E. Cripps, M. J. Emslie, M. Jonker, B. Schaffelke, and H. Sweatman, *Coral-macroalgal phase shifts or reef resilience: Links with diversity and functional roles of herbivorous fishes on the Great Barrier Reef*, Coral Reefs, 29(4):1005–1015, 2010.

[11] M. Chen, M. Fan, and Y. Kuang, *Global dynamics in a stoichiometric food chain model with two limiting nutrients*, Math. Biosci., 289(4):9–19, 2017.

[12] J. A. Cui and Y. Takeuchi, *Permanence, extinction and periodic solution of predator-prey system with Beddington-DeAngelis functional response*, J. Math. Anal. Appl., 317(2):464–474, 2006.

[13] L. P. Ding, B. X. Huang, and Y. Q. Xie, *Advances and problems with the study of marine macroalgae of China seas*, Biodiv. Sci., 19(6):798–804, 2011.

[14] P. J. Edmunds et al., *Persistence and change in community composition of reef corals through present, past, and future climates*, PLoS One, 9(10):e107525, 2014.

[15] M. Fan, I. Loladze, Y. Kuang, and J. J. Elser, *Dynamics of a stoichiometric discrete producer-grazer model*, J. Difference Equ. Appl., 11(4-5):347–364, 2005.

[16] T. Fung, R. M. Seymour, and C. R. Johnson, *Alternative stable states and phase shifts in coral reefs under anthropogenic stress*, Ecology, 92(4):967–982, 2011.

[17] R. González-De Zayas, S. Rossi, L. Hernández-Fernández, R. Velázquez-Ochoa, M. Soares, M. Merino-Ibarra, F. S. Castillo-Sandoval, and M. F. Soto-Jiménez, *Stable isotopes used to assess pollution impacts on coastal and marine ecosystems of Cuba and México*, Reg. Stud. Mar. Sci., 39:101413, 2020.

[18] M. González-Rivero, L. Yakob, and P. J. Mumby, *The role of sponge competition on coral reef alternative steady states*, Ecol. Model., 222(11):1847–1853, 2011.

[19] J. P. Grover, *Stoichiometry, herbivory and competition for nutrients: Simple models based on planktonic ecosystems*, J. Theor. Biol., 214(4):599–618, 2001.

[20] H. Hillebrand and V. Lehmpfuhl, *Resource stoichiometry and consumers control the biodiversity-productivity relationship in pelagic metacommunities*, Am. Nat., 178(2):171–181, 2011.

[21] C. A. Klausmeier, E. Litchman, and S. A. Levin, *Phytoplankton growth and stoichiometry under multiple nutrient limitation*, Limnol. Oceanogr., 49(4):1463–1470, 2004.

[22] B. E. Lapointe, R. A. Brewton, L. W. Herren, J. W. Porter, and C. Hu, *Nitrogen enrichment, altered stoichiometry, and coral reef decline at Looe Key, Florida Keys, USA: A 3-decade study*, Mar. Biol., 166(8):108, 2019.

[23] X. Li and H. Wang, *A stoichiometrically derived algal growth model and its global analysis*, Math. Biosci. Eng., 7(4):825–836, 2010.

[24] X. Li, H. Wang, and Y. Kuang, *Global analysis of a stoichiometric producer-grazer model with Holling type functional responses*, J. Math. Biol., 63(5):901–932, 2011.

[25] X. Li, H. Wang, Z. Zhang, and A. Hastings, *Mathematical analysis of coral reef models*, J. Math. Anal. Appl., 416(1):352–373, 2014.

[26] D. Lirman, *Competition between macroalgae and corals: Effects of herbivore exclusion and increased algal biomass on coral survivorship and growth*, Coral Reefs, 19(4):392–399, 2001.

[27] M. M. Littler and D. S. Littler, *Models of tropical reef biogenesis: The contribution of algae*, Prog. Phycol. Res., 3:323–364, 1984.

[28] M. M. Littler, D. S. Littler, and B. L. Brooks, *Harmful algae on tropical coral reefs: Bottom-up eutrophication and top-down herbivory*, Harmful Algae, 5(5):565–585, 2006.

[29] I. Loladze, Y. Kuang, and J. J. Elser, *Stoichiometry in producer-grazer systems: Linking energy flow with element cycling*, Bull. Math. Biol., 62(6):1137–1162, 2000.

[30] I. Loladze, Y. Kuang, J. J. Elser, and W. F. Fagan, *Competition and stoichiometry: Coexistence of two predators on one prey*, Theor. Popul. Biol., 65(1):1–15, 2004.

[31] L. McCook, J. Jompa, and G. Diaz-Pulido, *Competition between corals and algae on coral reefs: A review of evidence and mechanisms*, Coral Reefs, 19(4):400–417, 2001.

[32] J. W. McManus and J. F. Polsenberg, *Coral-algal phase shifts on coral reefs: Ecological and environmental aspects*, Prog. Oceanogr., 60(2-4):263–279, 2004.

[33] K. Mischaikow, H. Smith, and H. R. Thieme, *Asymptotically autonomous semiflows: Chain recurrence and Lyapunov functions*, Trans. Am. Math. Soc., 347(5):1669–1685, 1995.

[34] P. J. Mumby, N. L. Foster, and E. A. G. Fahy, *Patch dynamics of coral reef macroalgae under chronic and acute disturbance*, Coral Reefs, 24(4):681–692, 2005.

[35] P. J. Mumby, A. Hastings, and H. J. Edwards, *Thresholds and the resilience of Caribbean coral reefs*, Nature, 450(7166):98–101, 2007.

[36] G. P. D. Murray, R. A. Stillman, R. E. Gozlan, and J. R. Britton, *Experimental predictions of the functional response of a freshwater fish*, Ethology, 119(9):751–761, 2013.

[37] H. T. Odum and E. P. Odum, *Trophic structure and productivity of a windward coral reef community on Eniwetok atoll*, Ecol. Monogr., 25(3):291–320, 1955.

[38] N. Rädecker, C. Pogoreutz, C. R. Voolstra, J. Wiedenmann, and C. Wild, *Nitrogen cycling in corals: The key to understanding holobiont functioning?*, Trends Microbiol., 23(8):490–497, 2015.

[39] A. Rajasuriya, M. W. R. N. De Silva, and M. C. Öhman, *Coral reefs of Sri Lanka: Human disturbance and management issues*, Ambio, 24(7/8):428–437, 1995.

[40] L. A. Sanchez, *Convergence to equilibria in the Lorenz system via monotone methods*, J. Differential Equations, 217(2):341–362, 2005.

[41] I. H. Sarkar, J. Bhattacharyya, and S. Pal, *Herbivore harvesting and alternative steady states in coral reefs*, Appl. Math., 66:233–268, 2021.

[42] J. E. Smith, C. L. Hunter, and C. M. Smith, *The effects of top-down versus bottom-up control on benthic coral reef community structure*, Oecologia, 163(2):497–507, 2010.

[43] South China Sea Development Research Institute, MNR, South China Sea Ecological Center, MNR, China and South China Sea Survey Center, MNR, China, *A Survey Report on the Coral Reef Ecosystems of Tiexian Jiao and Niu'e Jiao*, 2025. `https://scs.mnr.gov.cn/scsb/shyw/202504/d1db93a508b74b3c8a6c5ed9df4d1536.shtml`

[44] R. W. Sterner and J. J. Elser, *Ecological Stoichiometry: The Biology of Elements from Molecules to the Biosphere*, Princeton University Press, 2003.

[45] R. W. Sterner and N. B. George, *Carbon, nitrogen, and phosphorus stoichiometry of cyprinid fishes*, Ecology, 81(1):127–140, 2000.

[46] T. H. Suchanek, R. C. Carpenter, J. D. Witman. and C. D. Harvell , *Sponges as important space competitors in deep Caribbean coral reef communities*, Symposia Series for Undersea Research, 1(1):55–60, 1983.

[47] M. F. Tan, G. J. Lan, and C. J. Wei, *Mathematical insights into the influence of delay and external recruitment on coral-macroalgae system*, J. Frankl. Inst., 361:107329, 2024.

[48] I. A. van de Leemput, T. P. Hughes, E. H. van Nes, and M. Scheffer, *Multiple feedbacks and the prevalence of alternate stable states on coral reefs*, Coral Reefs, 35(3):857–865, 2016.

[49] H. Wang, H. L. Smith, Y. Kuang, and J. J. Elser, *Dynamics of stoichiometric bacteria-algae interactions in the epilimnion*, SIAM J. Appl. Math., 68(2):503–522, 2002.

[50] N. Wang, L. Yang, and S. Q. Liu, *Stochastic dynamics of coral and macroalgae: Analyzing extinction and resilience in coral reef ecosystems*, Bull. Math. Biol., 87:99, 2025.

[51] R. Wood, *The changing biology of reef-building*, Palaios, 10(6):517–529, 1995.

[52] J. Wulff, *Assessing and monitoring coral reef sponges: Why and how?*, Bull. Mar. Sci., 69(2):831–846, 2001.

[53] T. Xie, X. S. Yang, X. Li, and H. Wang, *Complete global and bifurcation analysis of a stoichiometric predator-prey model*, J. Dynam. Differential Equations, 30(2):447–472, 2018.

[54] M. Zhang, *Asymptotic Behavior on Several Types of Coral Reef Ecosystem*, PhD Thesis, Shanghai Normal University, 2021.

[55] S. N. Zhao and S. L. Yuan, *A coral reef benthic system with grazing intensity and immigrated macroalgae in deterministic and stochastic environments*, Math. Biosci. Eng., 19(4):3449–3471, 2022.

[56] S. N. Zhao, S. L. Yuan, and H. Wang, *Threshold behavior in a stochastic algal growth model with stoichiometric constraints and seasonal variation*, J. Differential Equations, 268(9):5113–5139, 2020.

[57] X. Zhao, L. D. Liu, H. Wang, and M. Fan, *Ecological effects of predator harvesting and environmental noises on oceanic coral reefs*, Bull. Math. Biol., 85(7):59, 2023.

[58] X. Zhao, S. Y. Yu, and M. Fan, *Degradation of coral reef ecosystems: Mathematical-dynamical modeling approach*, EPL, 148:32001, 2024.

[59] X. Zhao, S. Y. Yu, and M. Fan, *White lies for coral reefs: Dynamics of two-patch coral reefs model with asymmetric dispersal*, J. Theor. Biol., 601:112046, 2025.